Climate Dynamics (2023) 61:2599–2621
https://doi.org/10.1007/s00382-023-06701-1

A cold wave of winter 2021 in central South America: characteristics and impacts

J. Marengo[1] · J. C. Espinoza[2] · L. Bettolli[3] · A. P. Cunha[1] · J. Molina-Carpio[4] · M. Skansi[5] · K. Correa[6] · A. M. Ramos[7] · R. Salinas[8] · J.-P. Sierra[2]

Received: 12 June 2022 / Accepted: 3 February 2023 / Published online: 16 February 2023

Abstract

During the austral winter (June–August) of 2021, the meteorological services of Brazil, Argentina, Peru, Paraguay, Bolivia, and Chile all issued forecasts for unusually cold conditions. Record-low minimum temperatures and cold spells were documented, including one strong cold wave episode that affected 5 countries. In this study, we define a *cold wave* as a period in which daily maximum and minimum air temperatures are below the corresponding climatological 10th percentile for three or more consecutive days. The intense cold wave event in the last week of June, 2021, resulted in record-breaking minimum daily temperatures in several places in central South America and Chile. Several locations had temperatures about 10 °C below average, central South America had freezing conditions, and southern Brazil even saw snow. The cold air surge was characterized by an intense upper-air trough located close to 35° S and 70° W. The southerly flow to the west of this trough brought very cold air northward into subtropical and tropical South America. A northward flow between the lower-level cyclonic and anticyclonic perturbations caused the intense southerly flow between the upper-level ridge and trough. This condition facilitated the inflow of near-surface cold air from southern Argentina into southeastern Brazil and tropical South America east of the Andes. In the city of São Paulo, the cold wave caused the death of 13 homeless people from hypothermia. Frost and snow across southern and southeastern Brazil caused significant damage to coffee, sugarcane, oranges, grapes, and other fruit and vegetable crops. Wine and coffee production fell, the latter by 30%, and prices of food and commodities in the region rose.

Keywords Cold waves · Minimum temperatures · Frost · Wave patterns · Coffee production

✉ J. Marengo
jose.marengo@cemaden.gov.br

1 Centro Nacional de Monitoramento e Alerta de Desastres Naturais, CEMADEN, Estrada Doutor Altino Bondensan, São José Dos Campos, São Paulo, Brazil

2 Institut des Géosciences de l'Environnement, Université Grenoble Alpes, IRD, CNRS, Grenoble, France

3 UBA, Universidad de Buenos Aires, Buenos Aires, Argentina

4 Universidad Mayor de San Andrés, Instituto de Hidraulica e Hidrología, La Paz, Bolivia

5 SMN, Servicio Meteorologico Nacional, SMN, Buenos Aires, Argentina

6 SENAMHI, Servicio Nacional de Meteorologia e Hidrologia, Lima, Peru

7 Instituto Nacional de Meteorologia, INMET, Brasilia, Brazil

8 Dirección de Meteorología e Hidrología/Dirección Nacional de Aeronáutica Civil, Asunción, Paraguay

1 Introduction

Cold surges involve the incursion of cold and dry air masses from the southernmost part of the continent of South America toward low latitudes (e.g., Sulca et al. 2018). A cold wave is a meteorological event generally characterized by a sharp drop of air temperature to extremely low values near the surface, a steep rise of pressure, and higher wind speed, associated with hazardous weather. However, worldwide consensus on a clear and consistent definition for cold wave events does not yet exist (WMO 2015). *Cold waves* are usually defined as persistent extreme low-temperature events sustaining specified temperatures below a certain threshold over a minimum number of days (Radinović and Ćurić, 2014; Peterson et al. 2013). This minimum temperature threshold depends on the geographical region and time of year. In some cases, cooling corresponds with—or is reinforced

by—widespread radiative cooling during a blocking and clear-sky atmospheric circulation (Garreaud 2000).

In South America, several observational and numerical studies have documented how cold surges can dramatically lower air temperature along their trajectory. Researchers have used observations and global reanalysis to document synoptic and dynamic characteristics of cold air surges in tropical South America east of the Andes. Typically, cold surges propagate towards the equator, and their path parallels the Andes Mountains and Brazilian highlands as they move northward (Garreaud and Wallace 1998; Garreaud 1999, 2000; Marengo et al. 1997a, 1997b, 2002; Krishnamurty et al. 1999; Espinoza et al. 2013; Lupo et al. 2001; Ricarte et al. 2015; Prince and Evans 2018; Sulca et al. 2018; Pezza and Ambrizzi 2005; Metz et al. 2013; Lindemann et al. 2021; and references quoted therein).

The large-scale circulation at middle and upper levels over South America during wintertime cold surges is characterized by a mid-latitude wave, with a ridge to the west of the Pacific coast of the continent, and a trough extending southeastward from the subtropics into the South Atlantic (Garreaud 1999). A resulting cold migratory anticyclone positions at the surface over the continent's southern tip in the southern Pacific. In addition, a deepening cyclone centered over the southwestern Atlantic grows, mainly due to upper-level vorticity advection (Marengo et al. 1997a). The surface anticyclone is supported by mid-tropospheric subsidence on the poleward side of a jet-entrance/confluent-flow region over subtropical South America. The northern edge of the anticyclone follows an anticyclonic path along the lee side of the Andes. It reaches tropical latitudes two to three days after its onset over southern Argentina (Garreaud 1999, 2000; Pezza and Ambrizzi 2005; Sicart et al. 2015; Segura et al. 2022). The concomitant cold air surges produce low-level cooling that can spread over the subtropical part of the continent, sometimes reaching western Amazonia as far north as 5° S (Marengo et al. 1997a; Espinoza et al. 2013). The associated cold front also induces atmospheric instability in the middle and upper troposphere.

Historical aspects of cold waves induced by cold surges in central South America from 1888 to 2003 are studied by Pezza and Ambrizzi (2005). These authors focus on extreme cold events in Argentina and southern Brazil, with data on snow accumulation in the mountainous regions of Rio Grande do Sul, Santa Catarina, São Paulo, Rio de Janeiro, and Minas Gerais. They also consider frost and black frost in the cities of São Paulo and Campinas, and events that caused widespread damage in Brazil's southeastern coffee-growing areas. Espinoza et al. (2013) define weather patterns from 1975 to 2001 in tropical South America related to cold surges reaching the Peruvian Amazon using ERA-40 reanalysis. They show that 52% of cold episodes registered in the southern La Plata basin propagate northward to the northern Peruvian Amazon at a speed of 20 ms^{-1}. Prince and Evans (2018) investigate cold surges that follow a path along the Andes Mountains from the middle latitudes to the tropics. They study austral winters (June–September) and identify 67 events between 1980 and 2017 using the ERA-Interim reanalyses. These events extend across the Amazon basin for up to eight days. Finally, Escobar et al. (2019) describe the climatology of cold surges between 1961 and 2012, using maximum and minimum temperatures of Cuiaba in central-west Brazil. Three to four cold surges are reported yearly (Brinkmann and Ribeiro 1972; Espinoza et al. 2013).

Case studies of intense cold surges in the Amazon region are the focus of several studies. In the western Amazon region, the locals call cold waves "friajes" or "surazos" (indicating the southerly direction of cold air) in Spanish-speaking countries (Espinoza et al. 2013), or "friagem" in Brazilian Portuguese (Serra and Ratisbona 1942; Marengo et al. 1997a, b). In early work, Morize (1922) and Myers (1964) study cold surges and cooling in Amazonia. Morize (1922) describes a June 1920 cooling event, when the temperature in northern Amazonia, close to Manaus in Brazil, dropped to 16 °C, causing the death of fish in lakes there. Myers (1964) investigates a cold air intrusion in 1957 that led to cooling in Amazonia, all the way to Venezuela, causing heavy rainfall and floods around 10° N. On July 19–20, 1975, minimum temperatures reached 8.0 °C in Pucallpa and 4.5 °C in Puerto Maldonado, in the Peruvian Amazon (where the long-term mean minimum temperatures for July are 21.0 °C and 18.1 °C, respectively; Marengo 1984). At the same time, minimum temperatures were almost 8 °C and 11.6 °C below average in Ji-Paraná and Rio Branco (in the southern Brazilian Amazon) (Marengo et al. 1997b). More recently, Camarinha-Neto et al. (2021) study the cold surge event of July 9–11, 2014, that reached the Amazon. They investigate changes in trace gas concentrations and atmospheric chemistry in the Amazon basin that accompanied this event, using data from the Amazon Tall Tower Observatory (ATTO) experimental site. These authors conclude that cold air intrusions could strongly interfere with microclimatic conditions and the atmosphere's chemical composition in the dense forest in the center of the Amazon basin.

Some individual cases with impacts on population and agriculture have been documented in recent decades (Hamilton and Tarifa 1978; Fortune and Kousky 1983; Marengo et al. 1997a, b; Garreaud 2000; Vera and Vigliarolo 2000; Marengo et al. 2002; Müller et al. 2005; Pezza and Ambrizzi 2005; Müller and Berri 2007; Espinoza et al. 2013; Muller et al. 2015). Perhaps the most intense episodes occurred in July 1975 and in June and July, 1994. In 1975, cold waves induced by surges of polar air were responsible for considerable losses in coffee production (estimated at USD $75 million), destroying almost 51% of Brazil's crop (Fortune and Kousky 1983; Marengo et al. 1997a). Willis (1976) reports

that the July 1975 cold wave harmed some species of local avifauna, and favored others, in the upper Paraguay basin and the southern Brazilian Amazon, thus affecting the ecosystem. The cold event of June 26, 1994, caused a sharp drop in coffee production and a dramatic price increase. That day, minimum temperatures reached − 1.0 °C in Londrina and Foz do Iguazu, in the State of Paraná, and frost burned most of the coffee fields (Marengo et al. 1997a). In July 2011, a cold event produced snow on the Altiplano of Chile, affecting grape and avocado production and exports (Mendonça and Romero 2012). In June 2018, the southern Peruvian Andes suffered heavy snowfall and cold conditions, substantially harming local people and their livelihoods (Bazo et al. 2021). Associated hazardous conditions, such as frost and ice, often cause severe impacts on human health, agriculture, and heating costs, even resulting in mortality for humans and livestock in central and southern South America (Lanfredi and Camargo 2018; Bazo et al. 2021).

Pezza and Ambrizzi (2005) show that extreme cold events, with record-low temperatures in Brazil and Argentina, have grown relatively less frequent, compared with previous decades. They also investigate how sea surface temperature (SST) in the Atlantic and South Pacific oceans and the sea ice cover around Antarctica affect the northward displacement of air. As for trends in cold and warm extremes, the frequency and intensity of extreme cold have decreased globally since 1950, with fewer cold nights in South America (Seneviratne et al. 2021). However, trends vary among studies, data sets, and regions (Dunn et al. 2020; Alexander et al. 2006; Donat et al. 2013). For example, Dunn et al. (2020) use the HADEX3 data set to identify a reduction of 1–2 days of cold conditions (TN10; cool nights, defined as a percentage of days with minimum temperatures below the 10th percentile) per decade from 1950 to 2018, mainly over Central America and tropical South America. Donat et al. (2013) find a similar trend using the HADEX2 data set for 1951–2010. They identify a slight, non-significant positive trend in the duration of cold spells over northern Argentina. In this region, and in southern Brazil and Paraguay, Balmaceda-Huarte et al. (2021) find significant downward trends in the frequency of cold nights and cold days (TX10; warm nights, defined as the percentage of days with a maximum temperature lower than the 10th percentile), relying on multiple observational data sets and reanalysis of the period from 1979 to 2017. Based on data from meteorological stations, Dereczynski et al. (2020) find stronger decreasing trends of TX10 and TN10 from 1969 to 2009 over Amazonia and northeastern Brazil than in southeastern and western South America. These results agree with those of Skansi et al. (2013), who also find significant reductions in cold spells from 1950 to 2010. Ceccherini et al. (2016) study the frequency of cold waves using the Global Surface Summary of the Day (GSOD) meteorological data set. They find no significant change in cold waves between 1980 and 2014 in southeastern South America.

In 2021, a few intense winter cold surges affected central South America and Chile. One of the most intense cold waves occurred in the last week of June and into July. It extended from western Amazonia and intensified towards southeastern Brazil. Its greatest intensity was in southern Brazil, Paraguay, Bolivia, northern Argentina, and central and southern Chile. The cold front passage under post-cold-front cold-core anticyclone conditions. Meteorological agencies reported these intense cold surges, accompanied by snow, hail, and freezing rain, in central South America and central and southern Chile during the last week of June, and from the second half of July to the beginning of August. In some cases, the cooling extended to northern Bolivia and the Peruvian Amazon, reaching lower latitudes. New historical record-low temperatures were measured in some locations east of the Andes, from western Amazonia to southeastern Brazil. Few people died due to the cold weather, but damage to crops was severe, mainly in the agricultural lands of south-central Brazil, Bolivia, and Paraguay. Based on the information available to date from state agencies, news media, and agricultural organizations, the cold waves in June and July 2021 were comparable, in terms of both intensity and of damage to agriculture (coffee, corn, and sugar cane production and prices), to the well-documented historical cases of June 1975 and June 1994 (Marengo et al. 1997a, b; WMO 2022).

In light of the history and documentation of past cold events in South America, this study comprehensively analyzes features of the cold spells and waves that affected central South America during the austral winter of June–August 2021. The study comprises Central South America, from the Amazon region to south-central Brazil, the Andean-Amazon regions of Bolivia and southern Peru, Paraguay, and northern Argentina. We investigate one cold wave that occurred during the last week of June 2021, assessing its intensity, spatial extension, and regional cooling patterns. This event affected all countries in central South America east of the Andes. We examine the daily variability of maximum and minimum temperatures from 36 meteorological stations to identify days with both cold waves and cold spells. In addition, we study regional and large-scale circulation patterns related to these cold waves. Finally, we discuss the local impacts of cold weather on human activities and long-term cooling trends in the region.

2 Data, data sources, and method

2.1 Data

For this study, we use both daily minimum and maximum surface air temperatures (T_{min} and T_{max}, respectively)

from 36 weather monitoring stations (Table 1, Fig. 1). The data are provided by the meteorological services of Brazil (INMET-www.inmet.gov.br), Bolivia (SENAMHI-senamhi.gob.bo), Paraguay (DMH-www.meteorologia.gov.py), Peru (SENAMHI-www.senamhi.gob.pe), and Argentina (SMN-www.smn.gob.ar). In addition, we use rainfall data from the Global Precipitation Climatology Center (GPCC-https://climatedataguide.ucar.edu/climate-data/gpcc-global-precipitation-climatology-centre). The GPCC gauge-based gridded precipitation dataset is available for the global land surface only and are available in the spatial resolutions of 1.0° latitude 1.0° longitude.

The focus of the study is the austral winter season from June to August 2021. Daily data allows day-to-day analysis

Table 1 Long term mean LTM climatology (1981–2010) of maximum and minimum temperature in stations from Central South America used in this study. (Source: Meteorological Services of Brazil, Bolivia, Argentina, Paraguay and Peru)

Station	Lat (°S)	Lon (°W)	Altitude (m)	June	July
Brazil				TMax/TMin (°C)	TMax/Tmin (°C)
1. Brasilia	15.79	47.93	1161	25.0/13.9	25.2/13.7
2. Goiania	16.67	49.26	749	29.7/14.3	30.1/14.2
3. Irati	25.50	50.64	882	19.8/8.9	19.9/7.9
4. São Paulo-M. Santana	23.50	46.62	785	22.5/13.0	22.4/12.3
5. Rio de Janeiro	22.86	43.41	31	26.5/19.3	26.0/18.7
6. Caxias do Sul	29.17	51.19	760	17.4/9.5	17.1/8.7
7. Rio Branco	9.96	67.87	160	30.4/18.3	31.3/17.5
Bolivia					
8. Ascensión de Guarayos	15.92	63.17	237	27.7/16.4	28.4/15.2
9. Puerto Suarez	18.98	57.82	134	26.9/17.1	27.2/16.1
10. San Ignacio de Velasco	16.38	60.96	416	27.4/14.7	28.3/13.4
11. Santa Cruz Trompillo	17.80	63.18	420	24.4/16.5	25.0/15.6
12. Riberalta	11.00	66.08	135	30.7/18.8	31.7/17.8
13. Yacuiba	21.97	63.65	646	21.0/9.8	22.3/8.3
14. San Joaquin	13.05	64.67	140	30.1/18.4	31.2/17.0
15. Cobija	11.04	68.78	235	30.1/17.7	30.8/16.7
Argentina					
16. Corrientes	27.47	58.84	62	21.0/11.6	21.1/10.4
17. Las Lomitas	24.70	60.61	130	23/4/11.8	24.1/10.4
18. Pdte Saenz Peña	26.78	60.43	93	21.8/11.1	22.2/9.7
19. Formosa	26.18	58.17	60	22.4/12.9	22.4/11.7
20. Obera	27.48	55.12	303	21.1/11.2	21.3/10.5
21. Resistencia	27.45	58.98	52	21.3/10.8	21.4/9.5
22. Iguazú	25.60	54.57	270	21.7/11.7	22.2/10.9
23. Posadas	27.36	55.89	125	21.9/12.4	21.9/12.0
24. Tinogasta	28.06	67.57	1201	19.9/0.8	19.8/0.2
25. Catamarca Aero	28.6	65.77	464	20.0/5.3	20.2/4.4
26. Jujuy Aero	24.38	65.08	907	19.7/6.8	20.3/5.8
Paraguay					
27. Mariscal Estigarribia	22.03	60.61	167	25.4/13.6	26.5/12.6
28. Puerto Casado	22.29	57.94	78	25.6/15.2	25.7/14.1
29. Pozo Colorado	23.49	58.79	98	25.2/15.4	25.8/12.7
30. Paraguari	25.62	57.14	116	23.4/10.0	23.9/11.9
31. Asunción	25.23	57.51	83	23.2/13.9	23.3/13.0
32. Concepción	23.44	57.43	75	25.1/14.3	25.4/13.0
33. Pilar	26.85	58.30	58	22.0/19.3	21.9/19.5
Peru					
34. Moyobamba	6.04	76.97	860	28.7/17.8	28.9/17.2
35. Puerto Inca	9.22	74.96	175	30.4/20.4	30.7/20.0
36. Amazonas	3.76	73.2	2334	30.7/22.3	31.3/21.9

Numbers in the first column to the left shows the location of the stations in Fig. 1

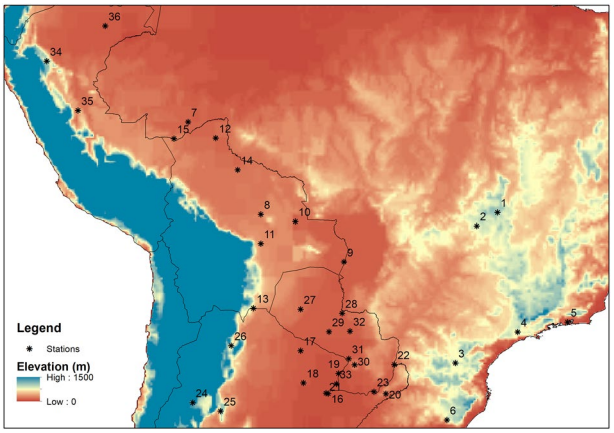

Fig. 1 Map showing locations of the 36 stations used in this study. Station number appears in the first column (left side) near the name of the station on Table 1

of temperature variability in central South America during cold-spell episodes, and identification of cold waves. The baseline for calculating anomalies is the 1981–2010 long-term mean (LTM). All these meteorological data come from the websites of the meteorological agencies, and are available upon request. Our study uses the daily minimum and maximum temperature and precipitation-gridded data from the NOAA Climate Prediction Center (CPC) (npsl.noaa.gov/data/gridded/data.cpc.globaltemp.html).

To corroborate the characteristics and impacts of cold waves in the winter of 2021, we rely on auxiliary information from weather reports issued by national meteorological services, from newspapers and other media reports, and from national and international agencies. Although the study region is central South America, we also consider information from Chile and northern Argentina. Central and southern Chile were affected by cold wave episodes from June to August 2021 due to the cold-core anticyclone as it approached South America. Therefore, we include information on cooling in some locations not listed in Table 1, from weather reports on the Chilean Meteorological Service's website (Dirección Meteorológica de Chile, www.meteochile.gob). More details on minimum temperature variability during cold waves in the wintertime of 2021 in other locations not in Table 1, from central South American countries and Chile, appear in supplementary material.

2.2 Definition of a cold wave or cold spell event

Considering the lack of a clear and consistent definition for cold wave and cold spell events around the world (WMO 2015), in this study we consider that a cold wave event is one that persists for at least three consecutive days with daily minimum and maximum temperatures (T_{min} and T_{max}) below the 10th percentile. If both T_{min} and T_{max} drop below the 10th percentile, but for fewer than three days, we use the term "cold spell".

We derive the daily threshold values for T_{min} and T_{max} from a 30-year climatological baseline period (1981–2010) in the CPC-NOAA dataset. Cold waves are detected in the June–August winter season.

2.3 Circulation fields related to cold waves

We learn from previous studies (see Sect. 1) that cold air surges arise from the meridional exchange of air masses between the tropics and mid-latitudes east of the Andes. These winter cold air surges may be responsible for frost events in this region of South America. Therefore, we wish to establish the relationship between surface cooling and lower- and upper-air circulation for the cold wave episode selected as a case study.

To study the surface synoptic circulation features for South America during the selected cold wave event from June to July 2021, we use the surface charts at the 00 GMT available from the Brazilian Navy (www.marinha.mil.br/chm/dados-do-smm-cartas-sinoticas/cartas-sinoticas). The 850- and 200-hPa winds and stream function variables show the Southern Hemisphere's large-scale circulation (cyclonic and anticyclonic anomalies) of the rotational component of the atmospheric flow. In addition, we consider 850-hPa temperature fields. The latest-generation reanalysis ERA5 allows us to analyze lower-level and upper-level large-scale atmospheric circulation and air temperature. The ERA5 reanalysis has a horizontal spatial resolution of 0.28° grid size, or ~ 30 km (Hersbach et al. 2020). We obtain daily means by averaging data available every 6 h for each variable of interest. We compute anomalies of horizontal winds and stream function at 850 hPa and 200 hPa for the June 26–July 1 case study of cold waves in the winter of 2021. For this analysis, we define a Day 0, which is strongly influenced by the cold core anticyclone that has crossed the Andes (high pressure anomalies centered over central Argentina; around 40° S and 70° W), and when the coldest day occurs in a region north of Paraguay (around 20° S and 60° W). Then, we go backward and forward to see the circulation patterns from 2 days before until 3 days after Day 0. Anomalies of streamfunction are calculated for these few days before and after Day 0. Since the coldest day is defined in northern Paraguay, and from the location and extension of the cold core anticyclone, we expect northward propagation (to the northwest along the Andes, and to the northeast towards southeast Brazil-Argentina) of the cold air in subsequent days. Anomalies are computed relative to the climatological mean from 1981 to 2010 for winter only.

To limit the fluctuation within a 30-day window, we apply a temporal high-pass Butterworth filter to the variables of interest. This filtering removes the seasonal cycle

and excludes variability due to the Madden–Julian Oscillation over this region (e.g., Alvarez et al. 2016; Mayta et al. 2018). In addition, the Butterworth filter allows us to control the sharpness of the cutoff on discarded frequencies, known as the order of the filter. Low order in the filter is related to a smooth-frequency cutoff (Roberts and Roberts 1978). In this work, we use the 5th order. This time-filter technique is widely used in meteorological sciences (e.g., Zeng et al. 2008; Berntell et al. 2018; Segura et al. 2022).

Because the extreme cold wave events occur due to a southerly cold air surge moving from higher latitudes, we examine the temporal evolution of surface meridional wind and temperature at 850 hPa from ERA-5 reanalyses for different locations between 9 and 29° S during the cold wave of June 26 to July 1, 2021.

3 Results

3.1 Maximum and minimum temperatures in central South America during June and July, 2021

Reports from national weather services of central South America and Chile, news, websites, United Nations organizations, and private meteorology companies (e.g., Climatempo in Brazil) identify cold episodes from June to August 2021: June 14–18, June 28 to July 4, and July 27–31. Some of these were later characterized as cold waves. In addition, some regions established new historical minimum temperature records and occurrence of frost and snow on these dates. Figure 2a–d shows anomaly maps for monthly minimum and maximum temperatures, and 2e–f shows rainfall anomalies for June and July 2021. In June, cold minimum temperature anomalies (0 to − 2 °C) occurred in a few locations in southern Brazil, Bolivia, Paraguay, and Argentina, while maximum temperatures were warmer than average in most of tropical South America. In July, the daily temperature amplitude was larger. Central, southern, and southeastern Brazil, Paraguay, parts of Bolivia, and northern and central Argentina exhibited negative minimum temperature anomalies (− 1 to − 4 °C). However, these regions also recorded positive maximum temperature anomalies (up to + 3 °C).

Rainfall anomalies can partially explain monthly temperature anomalies. Figure 2e shows anomalously wet conditions in southern Brazil and northern Argentina in June 2021, resulting in cloudier days, negative maximum- and minimum-temperature anomalies, and lower thermal amplitude. In July, anomalously warm and dry conditions in Bolivia, Paraguay, Argentina, and southwestern Brazil were related to the drought affecting the Paraná-Plata basin since 2019 (Naumann et al. 2021). Figure 2f suggests that drier-than-normal conditions over these regions in July 2021 resulted in clear skies during the day, allowing for more pronounced daily warming and nighttime cooling than usual.

Figure 3 shows the evolution of maximum and minimum temperatures between June and August 2021 in the 36 stations listed in Table 1 and displayed in Fig. 1. Lower minimum and maximum daily temperatures affected southeastern and central-western Brazil, southeastern Paraguay, eastern Bolivia, northern Argentina, and the southern Peruvian Amazon. For example, between June 28 and July 28, some days showed minimum and maximum temperatures 6–10 °C below the LTM (Table 1) in Argentina, Bolivia, Paraguay, and Brazil. In the Peruvian Amazon, the differences were about 3–5 °C. Three cold events were detected: June 13–16, June 26–July 4, and July 27–31 in Brazil, Argentina, Bolivia, and Paraguay. In the Peruvian Amazon, the latter two events were more intense. From June 15–21, 2021, Argentina reported a cold surge intrusion that lowered the temperature over much of the country, dropped snow in some regions, and set several new low-temperature records. However, the maximum temperature did not drop below the 10th percentile.

Later, on June 28 the minimum temperature dropped below the 10th percentile, thus meeting the definition of a cold spell rather than a cold wave. In the same period, news media reported frost conditions starting on June 20 that impacted coffee-growing areas in southeastern Brazil (Perfect Daily Grind PDG, 2021). In addition, the cold air mass moved over Brazil's agricultural areas by July 26, further damaging coffee and sugarcane crops already hurt by strong frosts the week before, and by the third consecutive year of drought. Finally, this cold wave brought freezing conditions to southeastern Brazil's agricultural belt, something not seen since 1994 (WMO 2022).

Reports from meteorological agencies and news media provide details of record-low temperatures at some weather stations in the five countries in central South America and Chile during June and July 2021. Thanks to a powerful cold air mass in the last half of June 2021, Argentina, Uruguay, Paraguay, Bolivia, and Brazil suffered extreme and unprecedented cold weather outbreaks, with historic snowfall across some regions. These reports corroborate the tendencies observed in Fig. 3. In Brazil, CLIMATEMPO and INMET reported that after the passage of the cold front on June 26, temperatures dropped in the southern Brazilian Amazon (Rio Branco in Fig. 3), and by June 28, central and southern Brazil, Uruguay, Argentina, and Paraguay saw the world's largest negative cold anomaly outside the poles. In Argentina, the SMN reported cold weather around June 19 in northeast Argentina, Bolivia, and Paraguay, while the cold waves were concentrated around June 26 and July 28. On June 27, cold spells and rare snow were reported in Buenos Aires and Santa Fe

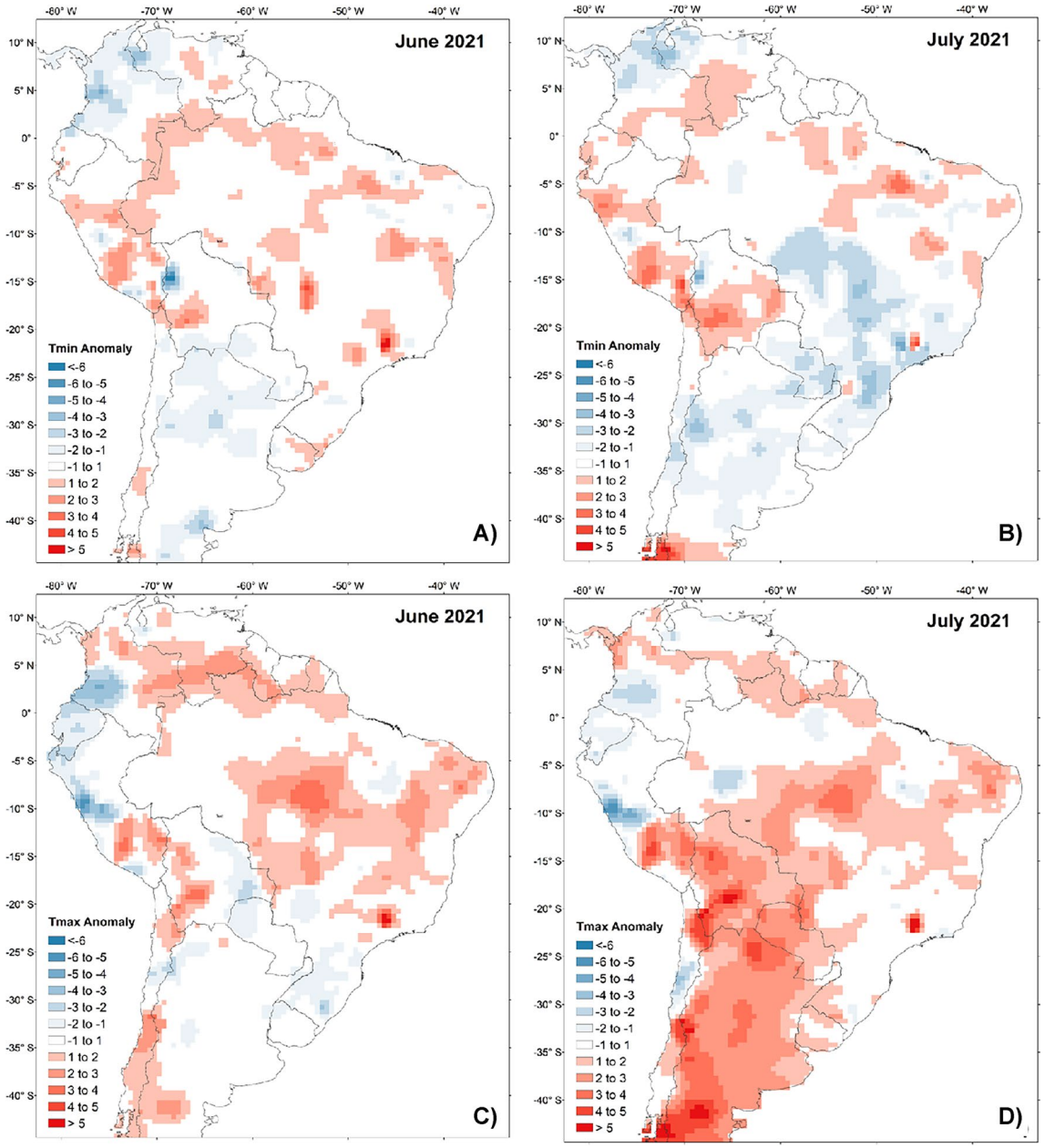

Fig. 2 Minimum temperature (T_{min} in °C) anomalies (**a**, **b**); Maximum temperature anomalies (T_{max} in °C) (**c**, **d**); and rainfall anomalies (**e**, **f**) for June and July 2021 (mm/month). Minimum and maximum temperature data comes from CPC, rainfall comes from the GPCC. Both temperature and rainfall anomalies are relative to the 1981–2010 LTM. Color scale is shown on the lower left side of the map (**a**–**d**) and on the lower side in panels **e**, **f**

provinces. The observatory in the capital registered 8.5 °C on June 27, followed by historic overnight lows. On June 28, several areas registered their coldest mornings of the year, including − 4 °C in Mendoza Aero, − 3.9 °C in Saint Martin, and − 6.9 °C in San Rafael. In Peru, SENAMHI reported on July 28 that minimum temperatures were around 13 °C in Puerto Inca in central Peruvian Amazonia. The Chilean Met service issued a forecast for cold weather in central Chile, and a cold wave from July 26–28 (see supplementary material for additional information on cooling during June and July 2021).

3.2 Identification of cold wave episodes

A cold wave is defined using the criteria explained in Sect. 2.2. Figure 4 identifies cold episodes between June 12 and August 31, 2021 for the 36 stations listed in Table 1. The black frame in a blue box delimits a cold wave event,

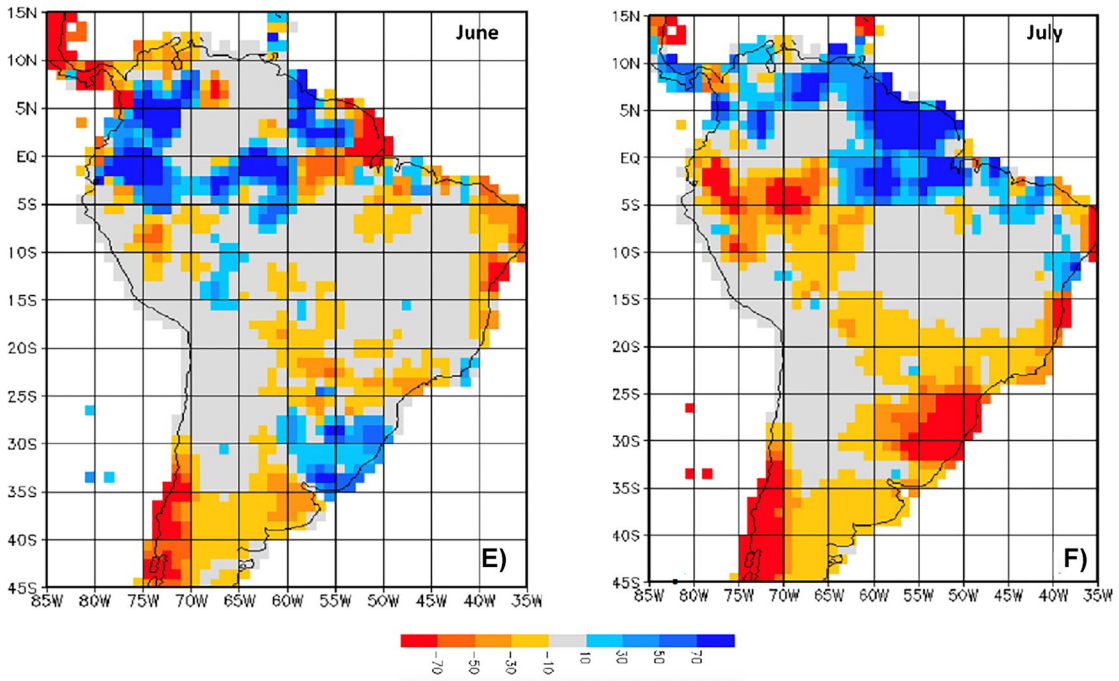

Fig. 2 (continued)

when daily minimum and maximum temperatures are below the corresponding climatological 10th percentile for at least three consecutive days. The blue box indicates when daily minimum and maximum temperatures are below the corresponding climatological 10th percentile, but for less than 3 days, representing cold spells. Cold waves (represented by red boxes in Fig. 4) were detected from June 26 to July 1 at 10 of the 36 stations, and from July 27 to 31 at 2 stations from Argentina. Cold waves were also detected in Paraguari (Paraguay) on June 17–19 and in Rio de Janeiro (Brazil) on August 12–14. The first wave was longer, affected five countries, and reached lower latitudes. This is consistent with the cooling observed at the station level from Fig. 3.

The first cold wave of winter 2021 lasted four days in Caxias do Sul (June 28–July 1). It lasted three days in southeastern Brazil (Rio de Janeiro, Irati) and in Rio Branco, in the western Brazilian Amazon (June 29–July 1). This cold wave also lasted three days in the Bolivian lowlands (June 28–July 1 in the southern and central regions, and June 29–July 2 in the north). In Argentina, the cold wave in Posadas lasted from June 28–30. Puerto Inca, in the central Peruvian Amazon, felt the cold wave later, on June 29–July 2 (SENAMHI-Peru). Figure 4 shows that only cold spells were detected on these dates in Paraguay, northern and central Argentina, and central-west Brazil. However, Paraguay's meteorological service reported cold waves from June 28 to 30 in several locations. On June 30, several places in Paraguay recorded their coldest temperatures ever: Mariscal Estigarribia (− 2.6 °C, LTM: 13.6 °C), Pozo Colorado (− 2.0 °C, LTM: 13.5 °C), and Aeropuerto Guarani (− 1.5 °C, LTM: 12.8 °C). Pedro Juan Caballero (1.0 °C, LTM: 13.4 °C) matched its previous 1.0 °C record-low from June 30, 1996 (Dirección de Meteorologia e Hidrologia-Paraguay). However, Fig. 4 does not show these events as cold waves. This is probably because cold waves in this country are defined based only on minimum daily temperatures below the 10th percentile, whereas our methodology requires both minimum and maximum temperatures below the 10th percentile for at last three consecutive days.

In Bolivia, coldest-ever temperatures were recorded on June 30 in Ascención de Guarayos (1.2 °C, LTM: 15.2 °C). Puerto Suárez matched its lowest-ever for June (1.0 °C, LTM: 17.1 °C). On July 4, Puerto Suárez in the Pantanal experienced its coldest temperature ever recorded (− 2.5 °C, LTM: 16.1 °C) (SENAMHI-Bolivia, Swiss Info 2021). First-ever or extremely rare frosts in the Chiquitania and Pantanal regions, between latitudes 16° S and 19° S, contributed to vegetation drying (and dying) in a context of an ecosystem (Chiquitano dry forest) already debilitated by the wildfires of previous years. All told, it was probably the most intense cold event of the last 50 years in those regions.

While some of these stations are listed in Table 1, we use additional information from other stations. Although not in Table 1, these stations' data are available from weather reports from SMN-Argentina, INMET-Brazil, DMH-Paraguay, SENAMHI-Bolivia, and SENAMHI-Peru. This

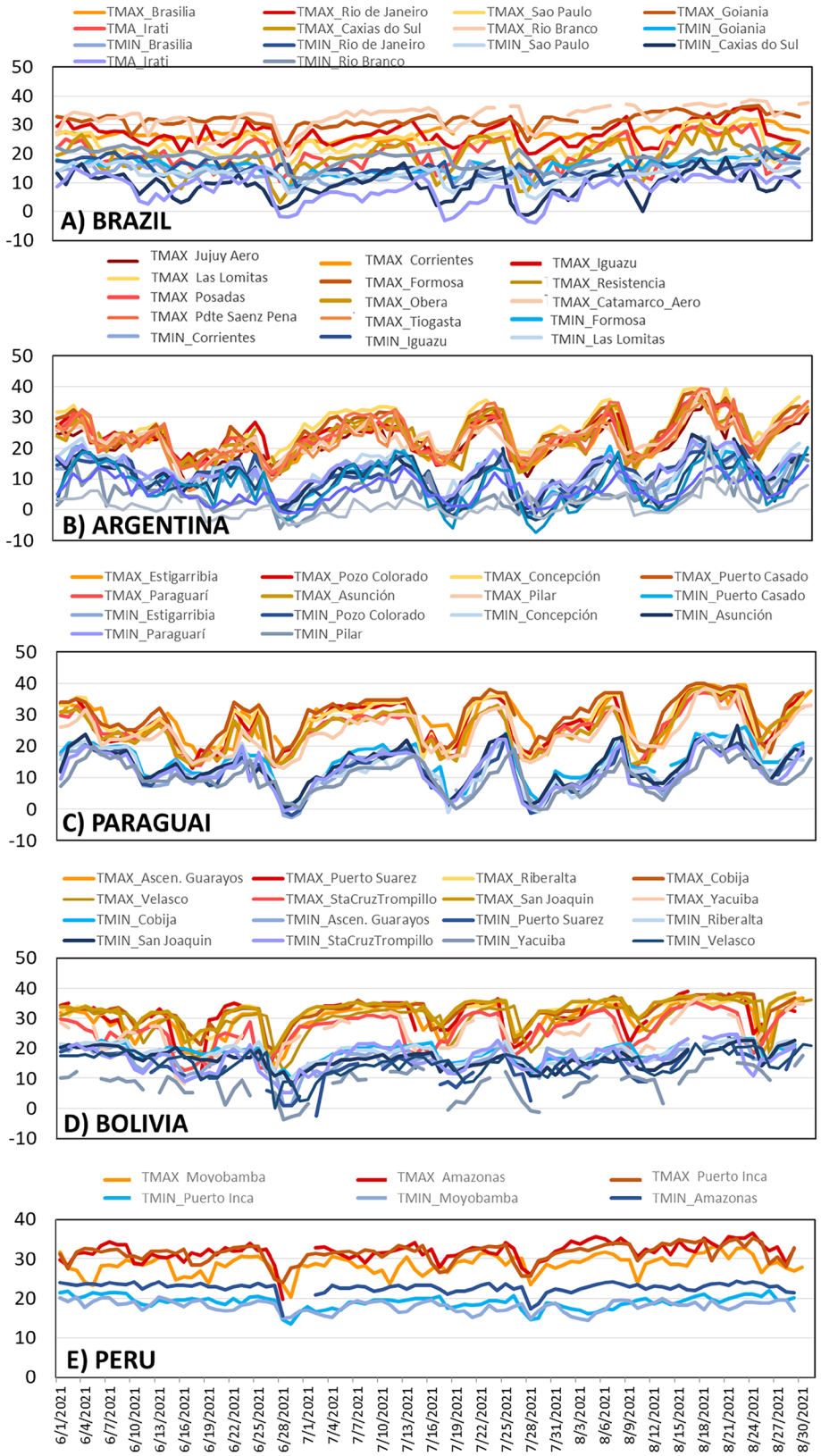

Fig. 3 Time series of minimum (T_{min} in °C) and maximum temperatures (T_{max} in °C) from June 1 to August 30, 2021, at stations in Argentina, Brazil, Paraguay, Bolivia, and Peru (Table 1). Sources of data: INMET (Brazil), SMN (Argentina), SENAMHI (Peru), SENAMHI (Bolivia), and DMH (Paraguay). Name of station is indicated above each panel

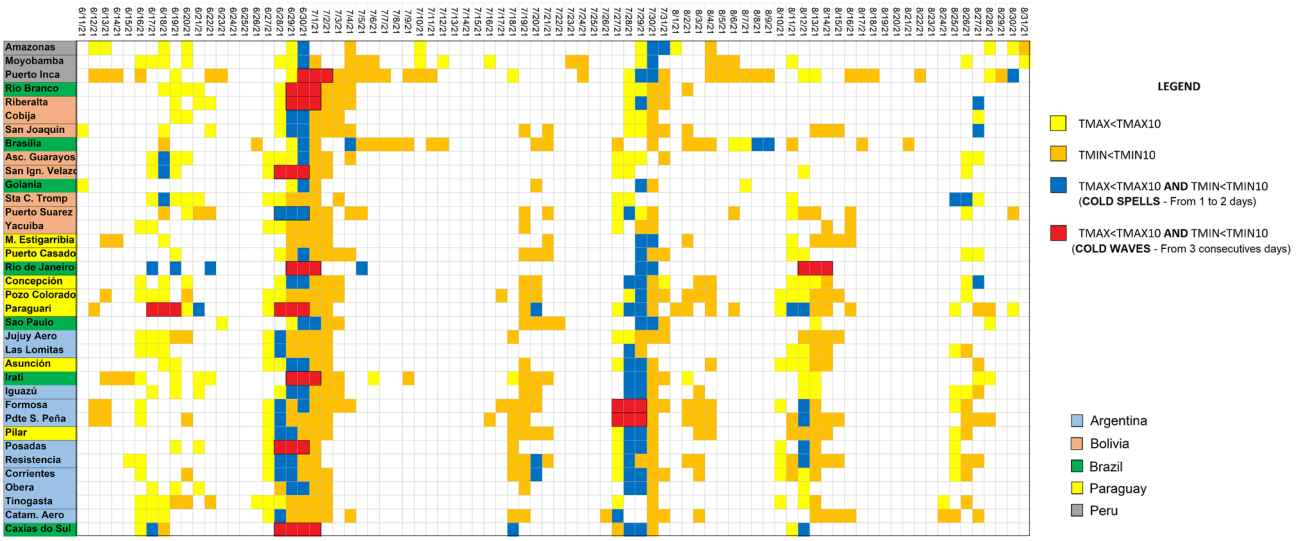

Fig. 4 Identification of cold waves (red boxes) and cold spells (blue boxes) based on the simultaneous occurrence of daily minimum and maximum temperatures below the corresponding climatological 10th percentile (Tmax10 and Tmin10) for weather stations in the study area. Stations from Argentina, Bolivia, Brazil, Paraguay and Peru are organized showing the northernmost stations at the top and southernmost stations at the bottom. Countries are indicated by color boxes. Geographical location of the stations is shown in Table 1 and Fig. 1

additional information provides a better picture of the degree and geographical extent of cooling in the region (in Sects. 3.2 and 3.3). This new information includes the daily minimum temperatures and the respective LTM (see Table S.1 in the supplementary material). Therefore, based on Fig. 4 and the additional information listed in the supplementary material, we define a case study of one cold wave period for further analysis, starting on June 26 and ending on July 1st.

From Figs. 3 and 4, the coldest day occurred between June 28 and 30 (Fig. 3). The cold wave began between June 28 and 29 (Fig. 4). The slight difference in dates is likely due to Fig. 3 using station data, and Fig. 4 the NOAA CPC gridded temperature data.

3.3 Regional climatic features of June 26–July 1, 2021

Figure 5a, b shows the minimum and maximum temperature anomalies at a regional level for this case study. From June 26 to July 1, anomalies extended from central and southern Brazil, central and northern Argentina, and Paraguay to eastern Bolivia, western Brazil, and the Peruvian Amazon, with maximum daily temperatures of 3–4 °C below average. Minimum daily temperatures of at least 4 °C less than baseline occurred in the same regions and extended further into central and southern Chile. During this cold wave episode, maximum daily temperature anomalies (at least − 4 °C lower than baseline) arose in southeastern Brazil, northern Argentina, and Paraguay. Anomalies in Bolivia and western Amazonia were from − 1 to − 3 °C. See the supplementary material for more information on minimum temperatures in other locations during this cold wave.

3.3.1 Cold wave of June 26–July 1, 2021

3.3.1.1 Synoptic surface features The synoptic charts of June 26–July 1, 2021, at 00 UTC (Fig. 6a–f) show that on June 26, a high-pressure system in the southern Pacific Ocean, with a maximum value of 1032 hPa, approached the coast of Chile and extended a weak ridge (green lines represent ridges) with its axis parallel to approximately 36° S latitude. Likewise, another ridge to the southwest advected cold air from high latitudes and supported the displacement of a cold front affecting southern Argentina. Further north, low pressure predominated over the continent. A deep extratropical cyclone associated with a cold front was seen in the southern Atlantic Ocean. On June 27, a migratory high-pressure system in the Pacific Ocean evolved (1034 hPa), crossed the Andes, and extended a ridge to its lee side. The system generated a strong northward transport of cold air in low layers of the atmosphere, reaching central and northern Argentina. In the extreme south of Brazil, on the coast of the Atlantic Ocean, a low-pressure system with minimum value of 1008 hPa was observed. The cold branch of a frontal wave, associated with it, affected the center-north of Paraguay's territory and southern Brazil.

On June 28, the center of the cold-core high-pressure system crossed the Andes, supporting the movement of the cold front separating the anticyclone from the warmer air

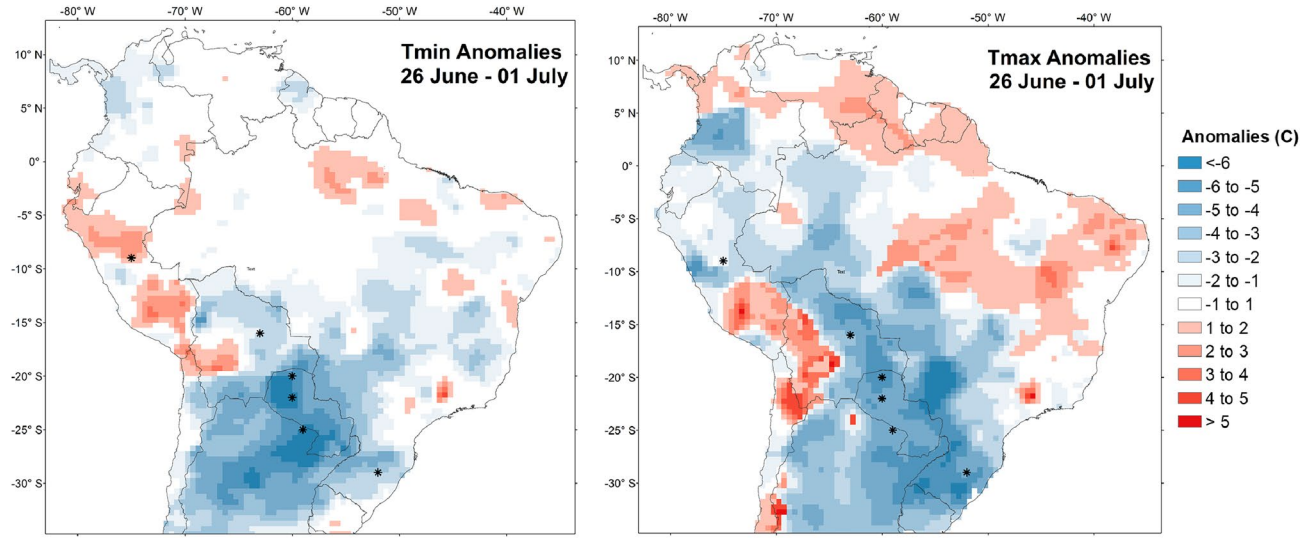

Fig. 5 Maximum and minimum temperatures (T_{max}, T_{min} in °C) anomalies (**a**, **b**) for the cold wave identified in Fig. 4 (June 26–July 1st). Data from CPC. Anomalies are relative to the 1981–2010 LTM. Color scale is shown to the right side of the panel. Black asterisks represent some points (grid boxes) where time series of temperature and meridional have been plotted in Fig. 10, for 23 June to 7 July 2021

located to the north of the system. An intense extratropical cyclone with a minimum value of 996 hPa was observed on the Atlantic coast between Argentina and southern Brazil. This system generated a strong pressure gradient over the continent, accelerating wind and cold-air advection from the south towards lower latitudes, breaking into the southern reaches of Bolivia's territory. On June 29, the center of the anticyclonic system was located over central Argentina. It extended a ridge to the northwest, transporting cold air to western Amazonia. On June 29 and 30, the cold core anticyclone reached 1032 hPa. It was located between 20–30° S on the coldest days. The extratropical cyclone on the coast of southern Brazil into northern Argentina continued to intensify. It reached a minimum value of 988 hPa, strengthening the southern component winds over the coast of Argentina, Uruguay, and southern Brazil. By June 30, this low-pressure center was named subtropical storm Raoni by the Brazilian Navy. With its associated polar vortex and extratropical cyclone, it produced snow and frost in southern and central Brazil (G1, 2022). This storm intensified by July 1. The low-pressure system on the coast of Uruguay and southern Brazil acted as a "pump," helping to quickly transport the cold air mass towards the north, reaching tropical latitudes. On that day, the high-pressure center moved over Paraguayan territory, and the axis of the system's ridge showed its highest amplitude, reaching latitude 5° S over the Peruvian Amazonia. The high-pressure system's position, the low cloudiness, and the strong nocturnal irradiation determined the low minimum temperature in most of central South America.

3.3.1.2 Near-surface temperature fields The 850-hPa air temperature field anomalies from June 26 to July 1 (Fig. 7a–f) should be analyzed together with Fig. 6a–f. Low temperatures appeared off the coast of Chile by June 26, around 40° S and 80° W over the southern Pacific and extreme southern South America (around 6 °C below average). As it crossed the Andes by June 27, the cold air was located over southern Argentina and Chile from 30 to 50° S. As it invariably does, the cold air wrapped around the southern portion of the Andes and propagated northeastward, east of the Andes, to remain stationary around 25° S with cooling reaching − 6 °C. On June 28, the coldest days over central Argentina, Paraguay, central and southern Brazil, and eastern Bolivia, the cold air extended to northwest Amazonia, western Amazonia, and the area of South America east of the Andes between 0 and 50° S. The cold air was propelled by the sub-tropical storm Raoni (cooling between − 8 °C in southern Brazil and − 4 °C over the Peruvian and Bolivian Amazon regions).

On June 29 and 30, the cooling diminished in southern and southeastern Brazil. Meanwhile, the cold air moved over the western Brazilian Amazon, even reaching the equator. Notably, warm anomalies appeared ahead of and behind the cold anomaly from June 26 to 28 (warming between 4 and 7 °C). High-latitude warming is a general characteristic of cold waves, not restricted to North and South America (e.g., Kanno et al. 2015; Yu et al. 2015).

In sum, Figs. 6a–e and 7a–e indicate that in the June 26–July 1st event, a cold-core anticyclone moved a cold air mass forward into lower latitudes off the coast of Chile. It crossed the Andes, and then, due to the pumping effect of a

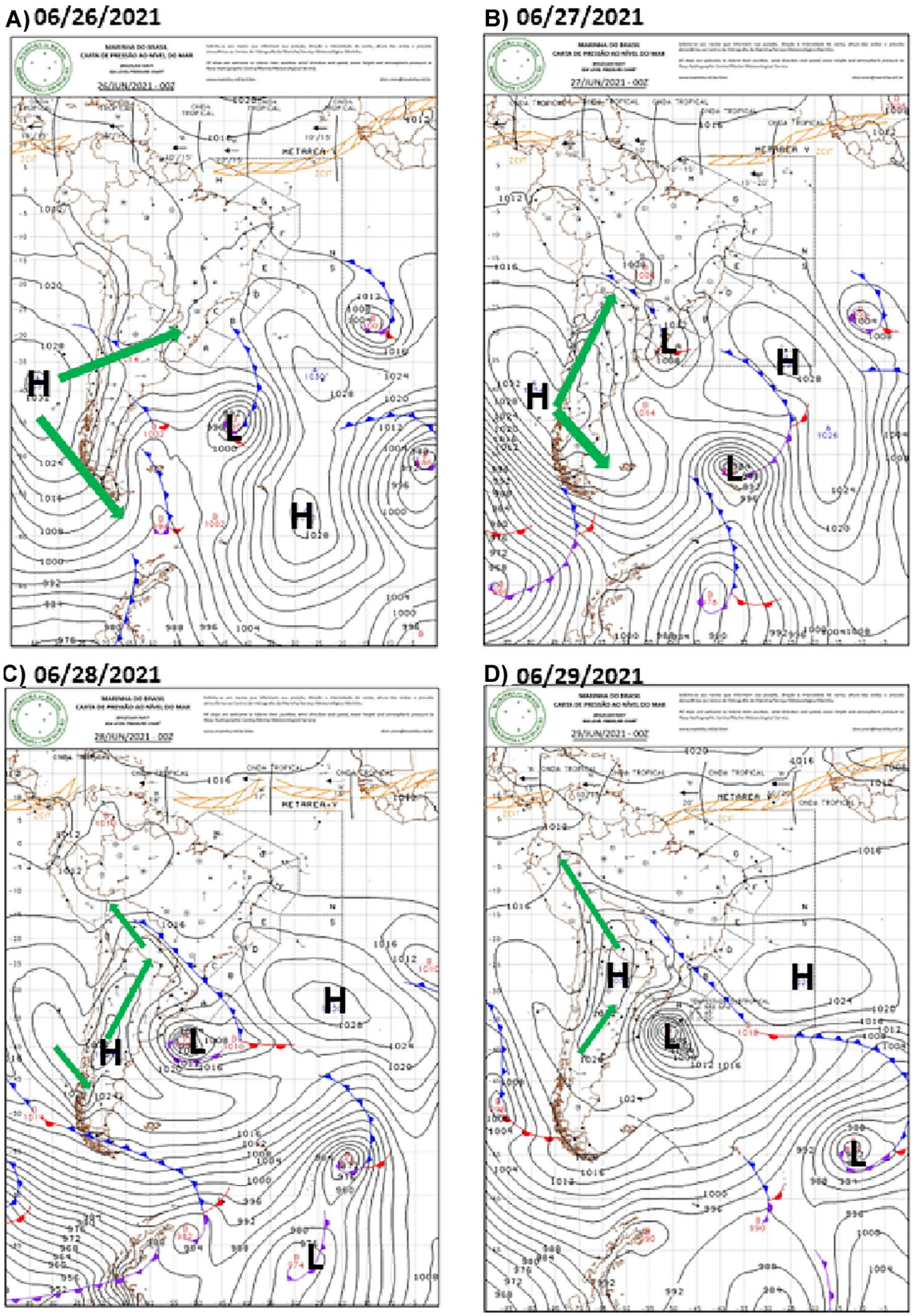

Fig. 6 Surface synoptic charts for South America, June 26–July 1 (**a**–**f**) for the 00 GMT. Maps provided by the Brazilian Navy Meteorological Department. Green arrows represent ridges as areas under the direct influence of the high-pressure system with the cold air incursion

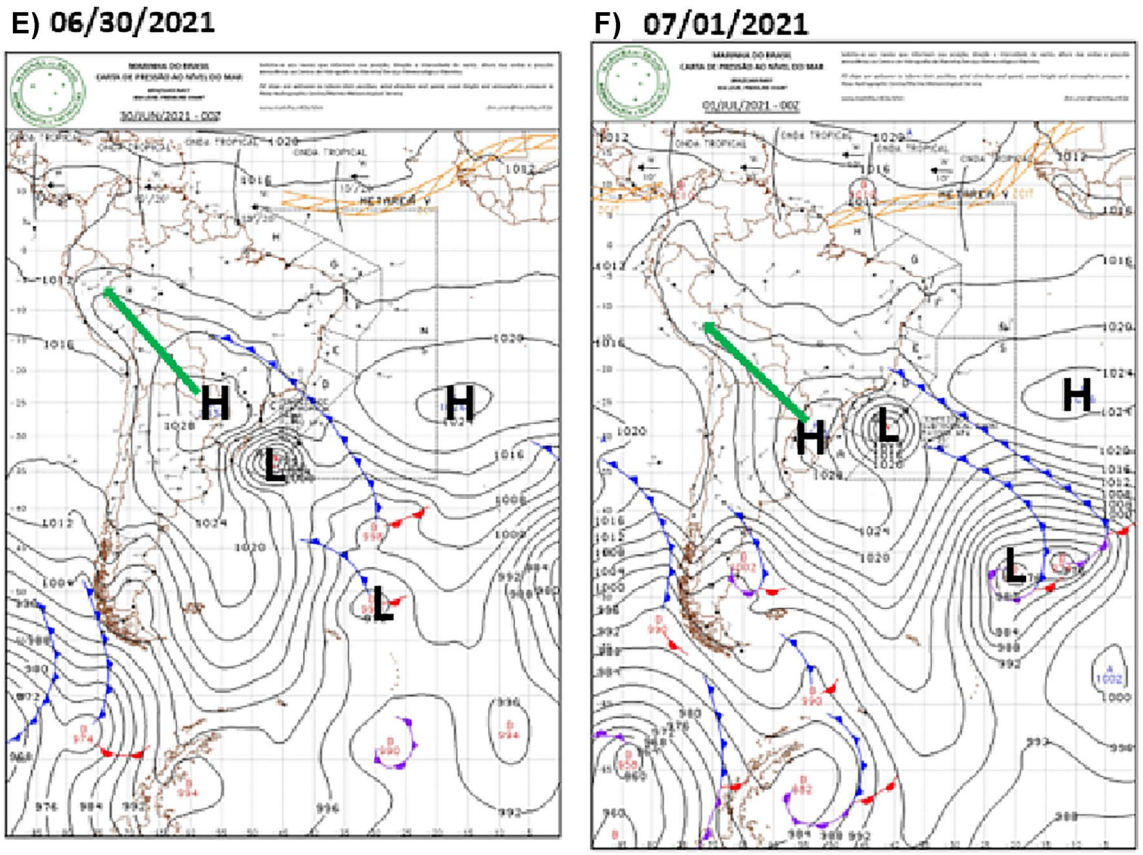

Fig. 6 (continued)

subtropical storm on the Atlantic, this cold air reached the equator by June 28 to 30. This pattern of cold air surges in tropical and subtropical South America east of the Andes is associated with large anticyclonic perturbations near the surface coming from the Pacific Ocean and wrapping around the Andes from the southwest. This is consistent with analysis of Marengo et al. (1997a, 2002), Garreaud (1999, 2000), Vera and Vigliarolo (2000), and Krishnamurti et al. (1999). Additionally, drought in 2021 (which had started in 2019 and would continue in 2022) affected most of central South America and the Paraná-La Plata basin. Some of the harm to regional agriculture was due to the combination of drought and cold events.

3.3.1.3 Large-scale circulation fields For high-level and low-level large-scale circulation and temperature and based on the dates of the occurrence of cold waves in southern Brazil and northern Paraguay, we select June 28 as Day 0. The 850 hPa stream function map (Fig. 9a–f) shows that cold air intrusions in tropical and subtropical South America east of the Andes accompanied the large anticyclonic perturbations near the surface coming from the Pacific Ocean and wrapping around the Andes from the southwest. This is consistent with Marengo et al. (1997a, 2002), Garreaud (1999, 2000), Vera and Vigliarolo (2000), and Krishnamurti et al. (1999). The June 26–30 cold wave followed a large anticyclonic perturbation around 100° W over the Pacific Ocean on Day − 4 (not shown) that approached the coast of South America (Fig. 9). This anomaly wrapped around the southern tip of the Andes from the southwest on Day − 2. It grew more intense on Day − 1 over the southern tip of South America; therefore, the conjoint of the horizontal vorticity advection and increased vorticity generation was due to column stretching/upward velocities (Marengo et al. 1997a). From Day − 1 to 0, the anomaly remained stationary over southern South America. Then, the signal of a high-pressure surge extended to tropical South America on Day + 1, with the anomalous southeasterly flow evident. The anomalous southeasterly flow to the east of the Andes had been observed in previous intense cold events in southern Brazil and is related to the channeling effect of the Andes (Garreaud 2000; Marengo et al. 2002).

These high-pressure eastward displacements have usually been related to mid-latitude Rossby wave trains originating from the westerly storm track in the South Pacific (Kiladis and Weickmann 1992; Ambrizzi and Hoskins 1997). By Day − 1, the anticyclonic near-surface anomaly wrapped around the southern tip of the Andes; it intensified on Day 0. On

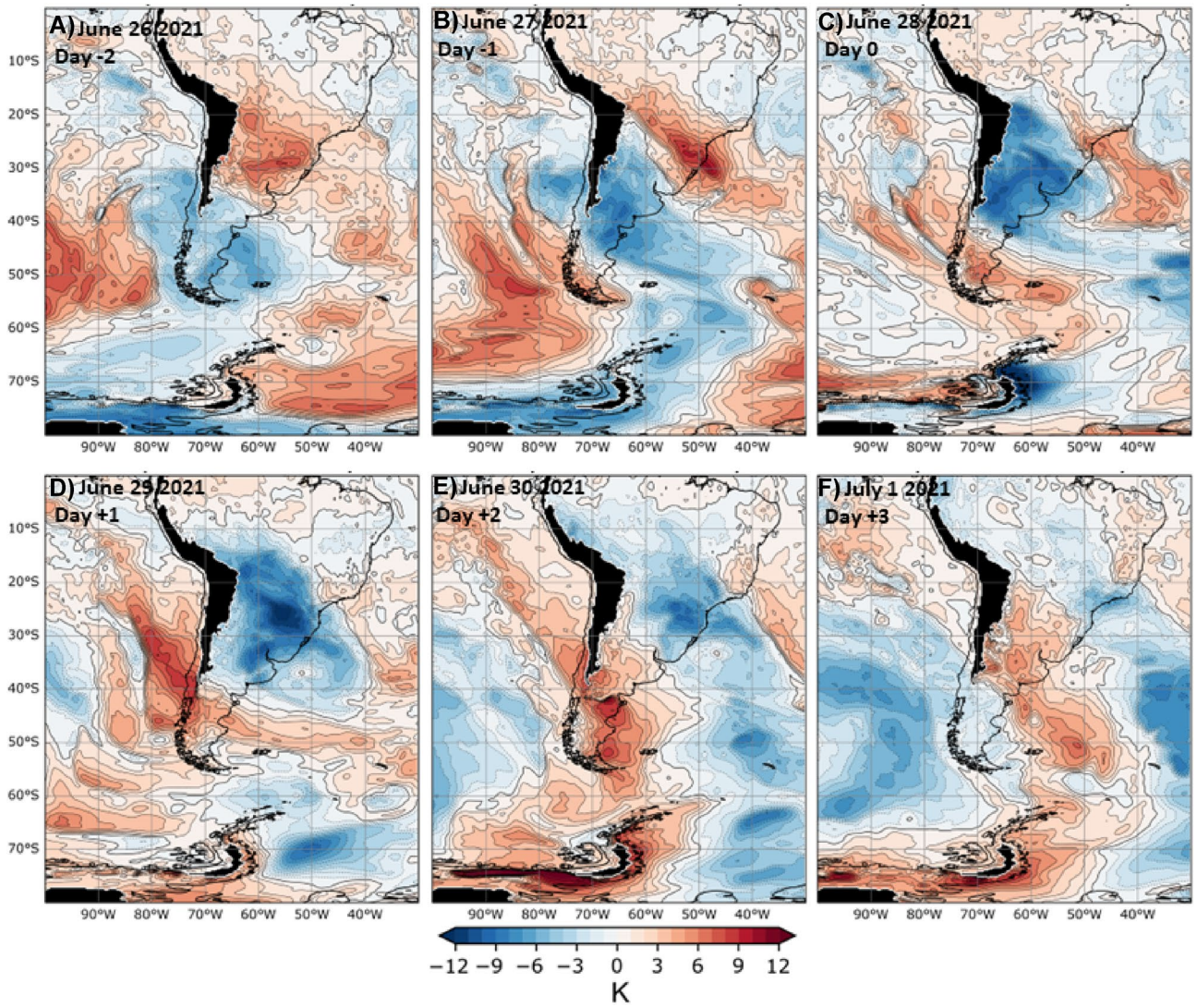

Fig. 7. 850 hPa air temperature anomalies (°C) for the cold wave of June 26–July 1 (**a**–**e**) for the 00 GMT. Blue/red colors depict areas with negative/positive temperature anomalies. Source: ERA-5 reanalyses

that day, an anticyclonic perturbation affected both sides of the Andes. Starting on Day 0, the high-pressure surge extended to the Amazon basin. Tropical South America is quite intense at the surface; an anomalous southeasterly flow emerged on Day + 2 and thereafter.

At the upper level (Fig. 8a–f), the 200-hPa stream function field's pattern was consistent with the near-surface signals. On Day − 6 (not shown), an anticyclonic perturbation was detected at 35° S 85° W. It intensified and approached Chile's coast by Day − 2. Right before this anomaly, a cyclonic perturbation (indicative of an upper-air trough) intensified over the southern tip of South America on Days − 6 and − 4 (not shown). We recognize this anticyclonic/cyclonic system as part of the eastward-moving Rossby wave train generated by a heating source over the tropical Indian and western Pacific Oceans (Marengo et al. 2002; Ambrizzi and Hoskins 1997). On Days − 2 and − 1, the ever-more-intense anticyclonic perturbation behind the cyclonic one moved to the east, crossing the Andes at around 45° S. From Days − 1 to + 1, the couplet of cyclonic/anticyclonic perturbations intensified. On Day 0, the cyclonic perturbation was located over northern Chile and Argentina, while the anticyclonic was over southern Chile and southern Argentina. Starting on Day + 1, the anticyclonic anomaly propagated to the east, while the cyclonic anomaly was over southern Brazil and northern Argentina. It moved northeast until Day + 3. The intensity of the stream function anomalies is typical of cold events in southern Brazil. Here, a ridge amplification at the upper levels extended to the west of the Andes and along the coast of Chile. A trough amplification spread over southern and southeastern Brazil. The northward flux between the cyclonic and anticyclonic perturbations also

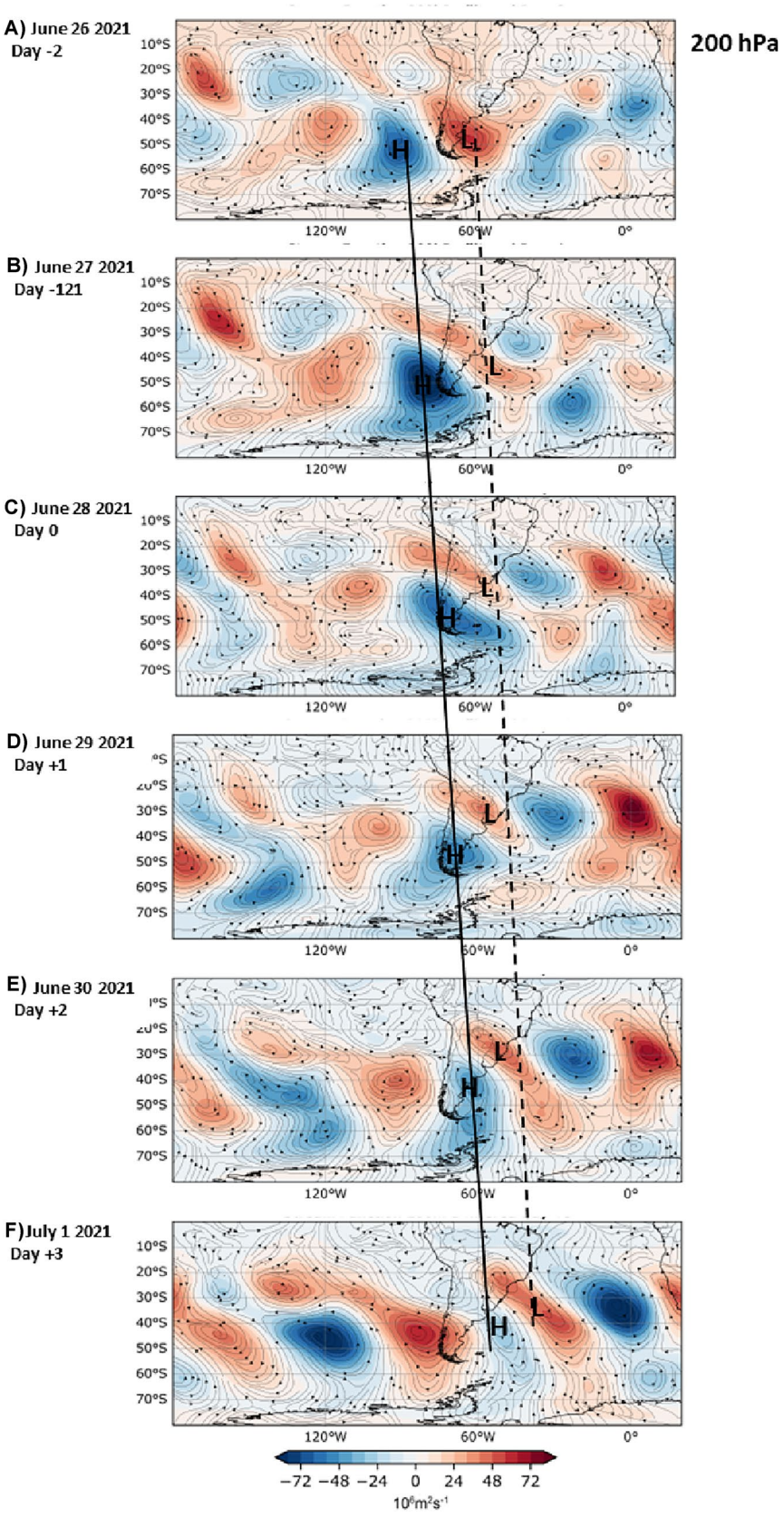

Fig. 8. 200 hPa (**a**–**f**) stream function (colors) and streamlines (lines) anomalies using the 1–30 day filtered horizontal winds for the extreme cold surge that triggered the cold wave June 28, 2021 (denoted as Day 0) for the 0000 GMT. Symbols − and + denote days prior to/after Day 0 of the event. Letters 'H' and 'L' represent areas with anticyclonic and cyclonic anomalies, respectively. Thick full and broken long lines show the approximate position of the ridge and trough, respectively. Source: ERA-5 reanalyses

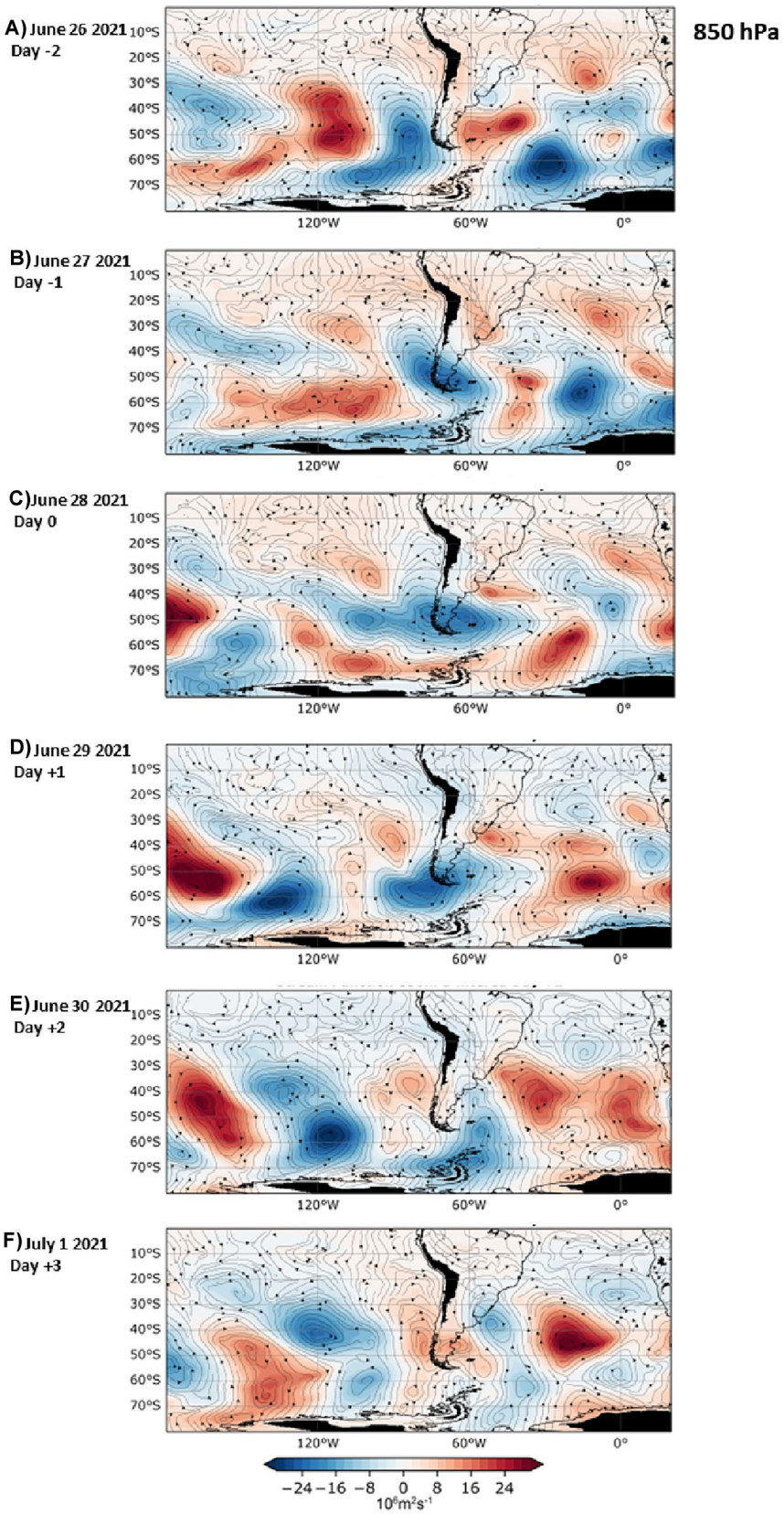

Fig. 9 As Fig. 8, but for 850 hPa

indicates the intense southerly flow between the ridge and trough, facilitating the inflow of near-surface cold air from southern Argentina into southeastern Brazil and tropical South America east of the Andes.

4 Discussion

In summary, Figs. 6, 7, 8 and 9 show that the cold wave identified in Fig. 4 was caused by a cold surge generated by an interaction between a cold-core anticyclone over the South Pacific and the intense cyclone in the South Atlantic. The large anticyclonic perturbations near the surface coming from the Pacific Ocean wrapped around the Andes at the southern tip of South America from the southwest, as observed 2–3 days before the coldest day in southern Brazil, and also observed in previous cold surges events (Espinoza et al. 2013). This interaction generated a strong pressure gradient in the western region of the cyclone, accelerating the southerly wind east of the Andes. This favored the advection of cold air from high latitudes to central South America. This advection was stronger during the end of June, due to the presence of the subtropical storm Raoni off the coast of Uruguay-Southern Brazil during the June 26–30 cold wave.

Regarding the air temperature anomaly fields from Fig. 7, a warm anomaly appeared 2 days before Day 0. After that, the warm anomaly decreased in intensity and was pushed to the north. While cold anomalies were located mainly over southeast Brazil in the second period in July, cold conditions in June had extended to low latitudes east of the Andes. They reached northwestern Amazonia on June 29–July 1. This is related to more intense southeast-northwest low-level winds over Amazonia in June. In this event, a warm anomaly appeared on the back of the cold air. This is analogous to cold surges in North America along the Rockies: Texas initially gets a cold surge, then the cold air advects eastward. Florida gets the freeze a few days later when Texas is already starting to warm up (Krishnamurti et al. 1999; Marengo et al. 2002).

Figures 8 and 9 show that southerly cold air incursions from June 26–July 1st were accompanied by a large-amplitude upper trough at mid-latitudes that extended deep into the tropics. This is detected in the 850- and 200-hPa stream function maps. Circulation on Day 0 was associated with an intense upper-air trough close to 35° S 70° W. The southerly flow to the west of this trough brought very cold air northward into subtropical South America. From Days − 1 to + 1, the couplet of cyclonic/anticyclonic perturbations intensified. On Day 0, the cyclonic perturbation was located over central Argentina, while the anticyclonic spread over southern Chile and southern Argentina. The vertical lines in Figs. 8 and 9 connect in time, illustrating the anticyclonic and cyclonic anomalies, like the downstream amplification mechanism shown by Krishnamurty et al. (1999). As in the case of June 25–26 1994 frost event in southeastern South America, it is likely that the end freeze event of the cold wave of June 26 to July 2, 2021 was related to the arrival of the ridge (located near 130° W).

The evolution of meridional wind and temperature during the cold wave of June 26–July 1 from ERA-5 reanalysis is assessed for some grid boxes: 9° S–75° W, 16° S–63° W, 20° S–60° W, 22° S–60° W, 25° S–59° W, and 29° S–52° W (Fig. 10). The figure shows the coldest day with an arrow. The letter S represents the southerly wind. Over the western Brazilian Amazon (9° S), the coldest day occurred on June 30, with 13 °C. In the Bolivian Amazon, (16° S), the coldest day was on June 29, with 8.5 °C. In northern and central Paraguay (20° S–22° S) the coldest day was June 28 (about 5 °C and 2 °C, respectively). In northern Argentina (25° S) and southern Brazil (29° S) the coldest day was June 29, with 1 °C and − 4 °C. The timing of the coldest day is consistent with the position of the cold core anticyclone (Fig. 6c,d); the ridge shows the flow of cold air to southern Brazil and northern Argentina on July 29. At lower latitudes (9° S), cooling is consistent with southerly flow starting July 29, and at 16° S from June 28. In both places, the coldest day occurred when the southerly wind reached its maximum. At the other locations, cooling accompanied southerly winds, and the maxima occurred either the day before or the day after the coldest day. Therefore, the southerly wind started to appear 1–2 days before the coldest day. The winds and the drop in temperature were both more intense in mid-latitudes, compared to lower latitudes.

5 Impacts of the cold wave of June 26–July 1, 2021

Frosts and snowfall in southern and southeastern Brazil in 2021 affected coffee, sugarcane, vegetable, and fruit crops. Production fell by 30%, and prices of food and commodities rose (Reuters 2021). Average temperatures in southeastern Brazil, a major coffee-producing region, fell to as low as − 1.2 °C, causing devastating, irreparable damage to coffee plants. The most heavily impacted regions were the states of São Paulo and Minas Gerais—the two largest coffee-producing states in Brazil. Around the world, market analysts and coffee traders suggest this could be the worst frost since 1994. They warn that repercussions for the global coffee market may last up to four years (Perfect Daily Grind PDG, 2021).

The severe frosts in the last week of July 2021 damaged many of the main Brazilian coffee fields. Preliminary estimates from the Brazilian government's food supply agency CONAB (www.conab.gov.br) indicate that these frosts affected 150,000 to 200,000 hectares—about 11% of the

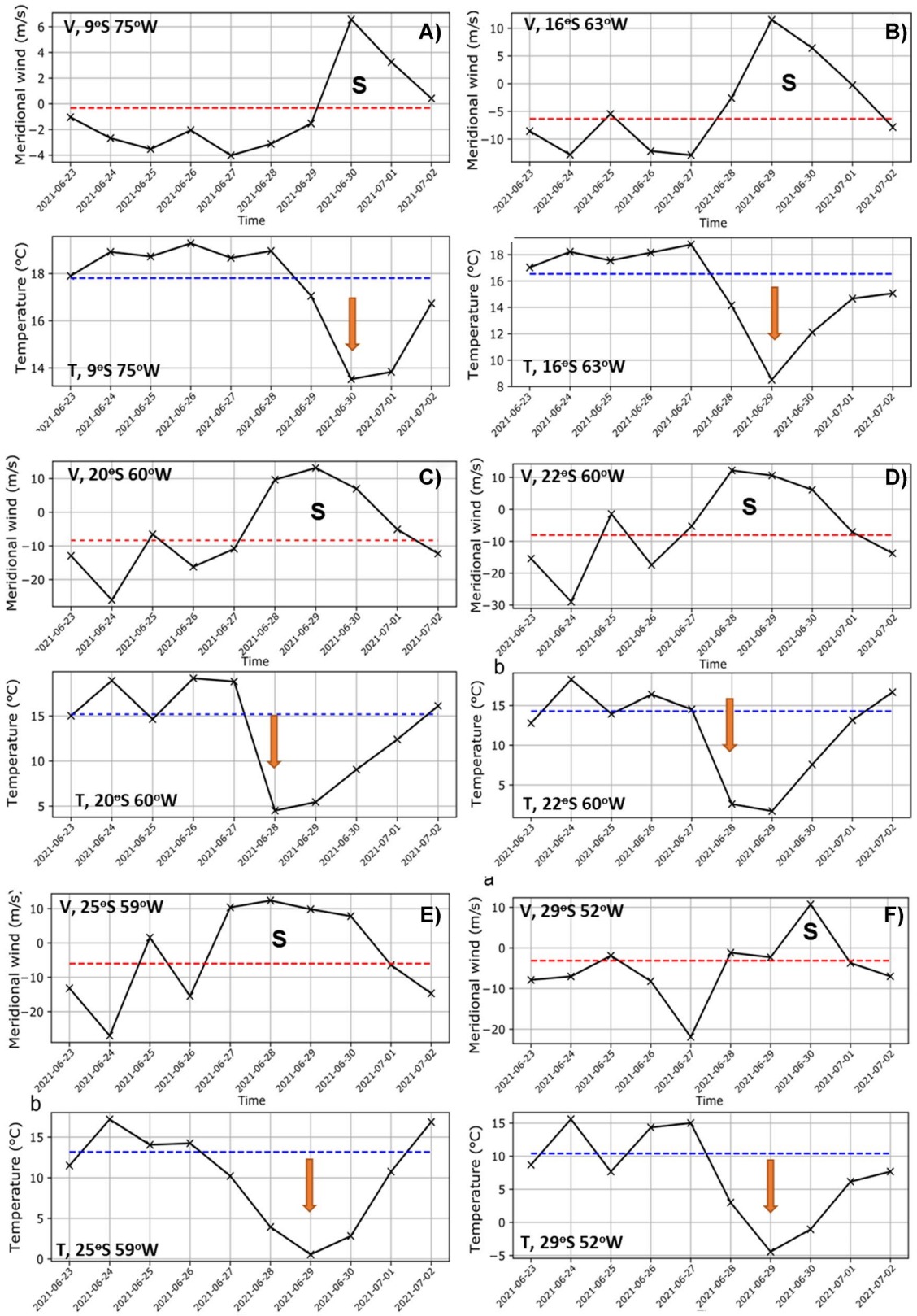
V, 9°S 75°W
A)
S
Meridional wind (m/s)
T, 9°S 75°W
Temperature (°C)
V, 16°S 63°W
B)
T, 16°S 63°W
V, 20°S 60°W
C)
T, 20°S 60°W
V, 22°S 60°W
D)
T, 22°S 60°W
V, 25°S 59°W
E)
T, 25°S 59°W
V, 29°S 52°W
F)
T, 29°S 52°W
Time

◂**Fig. 10** Time series of 850 hPa meridional wind and air temperature at 6 points (shown in Fig. 5) in different latitudinal bands in central South America east of the Andes: 9° S, 75° W; 16° S, 63° W; 20° S, 60° W; 22° S, 60° W; 25° S, 59° W; and 29° S, 52° W. June 23 to July 2, 2021. Red and blue broken lines show the 1981–2010 long term mean for meridional wind (m/s) and air temperature (° C) for June. The coldest day is identified with an arrow. Source: ERA-5 reanalyses

country's total arabica crop area (Reuters 2021). This marks the first time since 1994 that the country has experienced such a weather event. Current reasonable estimates suggest that anywhere from 2.5 to 5.5 million bags of coffee were lost. However, an accurate figure could be as high as 10 million bags (Perfect Daily Grind PDG, 2021).

After severe frosts during the last 2 weeks of July 2021, the price of coffee closed on Monday, July 26, above $2/lb. In U.S. dollars—the highest value since October 2014. However, cold weather damage is not the only reason prices have increased recently. Over 18 months, shipping container shortages, the Covid-19 pandemic, and protest blockades in Colombia also contributed to rising coffee prices (Perfect Daily Grind PDG, 2021).

Adding to the losses from the 2021 drought, frost-related losses may represent one of the biggest disasters for farms in recent years. These losses may total billions of Reais (Ministry of Agriculture, Livestock and Supply MAPA-www.gov.br/pt-br/orgaos/ministerio-da-Agricultura-pecuaria-e-abastecimento). By July 23, large agricultural areas in Minas Gerais were affected by frost. The Minas Gerais Agriculture Federation (FAEMG-www.sistemafaemg.org.br/faemg) announced that the region hit hardest was the southern part of the state, where the damage was described as "the worst in 27 years, after 1994." The Minas Gerais Agricultural Research Corporation (EPAMIG-www.epamig.b/) estimates that 30% of the area was damaged by frost and fires. In Mato Grosso do Sul, corn crops also suffered from the intense cold.

CONAB has already pointed out that the second harvest of 2020/2021, for which totals are not yet available, may suffer a drop of up to 30% in productivity. Consulting market analysts warn of an impending shortage of corn domestically in the second half of 2022. Imports will be necessary to fund the production chain. The sugar-energy sector had also already accumulated losses due to drought since 2021. CIIAGRO (www.ciiagro.sp.gov.br) advises that the sequence of polar air with heavy to severe frost further worsened the situation. CONAB estimates the 2021/2022 sugarcane harvest at 574.8 million tons, 4.6% lower than the previous harvest. Frost-related losses and accumulated losses from the 2021 drought ranked among the biggest disasters for Brazilian farmers in recent years. CONAB estimates that coffee production in Brazil in 2022 will be 120,000 tons lower than had been forecasted in May 2021, due to 2021's cold waves and drought (WMO 2022).

6 Conclusions

This study characterizes the climatic and large-scale meteorological patterns of an intense cold wave that affected central South America from June to July 2021. As the incursion of cold air advanced toward tropical South America, cooling was felt even in low latitudes, including in western Amazonia. In the western Brazilian Amazon and northern Bolivia, minimum temperatures of between 7 and 10 °C were observed (almost 10 °C below average). Sub-zero temperatures were recorded in southern Brazil, southern Bolivia, Paraguay, and northern Argentina. First-ever or very unusual frosts were recorded in Bolivia's Chiquitania and Pantanal regions, causing further damage to vegetation already debilitated by previous years' wildfires, and causing significant crop and crop-related losses in southern and southeastern Brazil. Around 1–2 days before the cold waves reached lower latitudes in central South America, cooling was already felt in central and southern Chile.

The cold surges were due to the action of (a) the cold-core anticyclone that approached central-southern Chile, crossed the Andes at the tip of South America, and wrapped around the Andes, and (b) the deepening cyclone centered over the southwestern Atlantic supported by upper-level vorticity advection. The pressure gradient generated by these two systems forced the air to move northerly along the Andes, reaching central South America in a few days. The June 26–July 1st case study shows that in addition to the anticyclone over the south Pacific and the cyclone over the South Atlantic, another factor emerges. A low-pressure system, the subtropical cyclone Raoni, formed off the coast of southern Brazil and Argentina on June 27. It intensified until June 29, pumping cold air until 5° S along with the cold air advection along the Argentinean Andes.

In the winter of 2021, the combination of cold temperatures and dry conditions reported since 2019 in the Paraná-La Plata basin in southern South America presented an extreme-cold and drought compound event. This impacted regional agriculture, particularly affecting commodities such as soybean, corn, and sugar cane in southeast Brazil (WMO 2022). In São Paulo, 13 homeless people died due to hypothermia. In addition, new historical minimum temperature records were registered in meteorological stations of Bolivia, Peru, and Brazil during these cold waves.

According to Lupo et al. (2001), cold surges in South America follow three main trajectories: (a) along the Atlantic coast, (b) along the Paraná River axis, and the (c) between the Brazilian Shield and the eastern flank of the Andes. After analyzing Figs. 6, 7, 8 and 9, we show that the June 26–July 1, 2021, cold wave followed trajectory

(c). By the end of June 2021, the cooling reached the equator and affected western Amazonia, mainly due to the action of a subtropical storm.

The intensity of the cold-core anticyclone that crossed the Andes at the southern tip of South America, and that remained stationary around 20–30° S during the coldest days, was relatively lower than those of the cold waves of July 1975 and June 1994. For example, during the intense cold wave of June 23–26, 1994, the cold core anticyclone reached reached Paraguay on June 26 with an intensity of 1036 hPa (Krishnamurty et al. 1999). Minimum temperatures in São Paulo reached 2.5 °C on June 26, and Rio Branco reached 12.3 °C on June 27, 1994 (Marengo et al. 1997a). On July 17, 1975, the cold core anticyclone was located at around 25° S with an intensity of 1044 hPa over northern Argentina–Paraguay, and air temperatures behind the cold front dropped to 0 °C north of 21° S (Parmenter 1976). On June 28–29, 2021, the cold core anticyclone reached 25–30° S with an intensity of 1032 hPa. While in this paper we used synoptic charts from the Brazilian Navy for the 0000 GMT, the early study by Parmenter (1976) used the National Meteorological Center (NMC) for the 1200 GMT for July 1975. On the other hand, Krishnamurty et al. (1999) used synoptic charts from the INMET (National Institute for Meteorology of Brazil) and from the National Center for Environmental Predictions (NCEP) for 0000 and 1200 GMT for June 1994.

Our analysis of lower- and upper-level circulation fields shows that the cold wave of June 26–July 1, 2021, were accompanied by a large-amplitude upper trough at mid-latitudes extending further into the tropics. The coldest day, June 28, had an intense upper-air trough close to 35° S, 70° W. The southerly flow west of this trough brought cold air northward into subtropical and tropical South America. Intense stream function anomalies are typical of cold events in southern Brazil, where a ridge amplification exists at the upper levels to the west of the Andes along the Chilean coast, and a trough amplification occurs over southern and southeastern Brazil. The northward flow between the low- and high-pressure systems and lower and higher levels also indicates the intense southerly flow between the ridge and trough. This facilitates the inflow of near-surface cold air from southern Argentina into southeastern Brazil, in tropical South America east of the Andes. The extreme cold wave occurred due to extremely strong southerly wind together with extremely cold airmass from the cold-core anticyclone located around 30° S and 62° W.

This is consistent with the 200-hPa stream function fields, where the ridge/trough represented by the anticyclonic/cyclonic stream function anomalies were particularly intense from Day -1 to Day + 1 in both events. We attempt to associate the intensity of cold surges in central South America with the location and intensity of their sources in the west Pacific. We show that during austral wintertime, Rossby wave activity that originates in the west Pacific propagates towards the west coast of southernmost South America, in a way similar to the patterns discussed by Muller et al. (2015). It then moves towards the equator to the east of the Andes, generating cold surges as it goes. Orographic effects must always be considered to explain this meteorological phenomenon and its variations. On the coldest day in southern Brazil, the southerly meridional wind was about 10–13 m/s above average, and the air temperature dropped to about 5 °C on Day 0. At 9° S, the coldest day occurred 2 days later, but both cooling and southerly wind decreased.

In addition, according to NCEP Global Forecasting System GFS and CSFR reanalyses, in June and July 2021, the south pole was colder than usual, with strong cold anomalies over much of Antarctica. In addition, the Southern Annular Mode (SAM) during the positive phase is associated with colder temperatures over southern Brazil in summer and spring (Campitelli et al. 2021). In the negative SAM phase, the wind belt weakens and moves north towards the equator, and the subtropical jet, which works as a waveguide, drifts northward and favors cyclone propagation towards southeast South America. The greater swell of the jet stream in the negative phase favors cyclone and anticyclone propagation towards southeast South America. The impact seems to be more important on the cyclones and depending on the signal of the SAM they may propagate northward (negative SAM phase-Reboita et al. 2009). Because of this, chances of more extreme cold events occurring in the Southern Cone of America (Carvalho et al. 2005; Reboita et al. 2009) increase. In mid-June 2021, the SAM entered a negative phase, which favored incursions of very cold air at mid-latitudes such as Brazil, a favorable scenario for more intense cold waves in more southern countries of the Southern Hemisphere. These colder conditions also influenced the sea ice around Antarctica. According to data from the European Copernicus system (www.copernicus.eu/en/access-data), the ice pattern observed in the winter of 2021 showed a concentration of sea ice with higher-than-normal values west of the Antarctic peninsula, north of the Bellingshausen and Amundsen seas. Kumar et al. (2021) reveals a strong relationship between sea-ice variability and ocean-atmospheric forcings. These relationships are not constant over time; so, continuous monitoring is required. While it is not among the objectives of this study to investigate associations between cold waves and teleconnection patterns such as the SAM, this remains as an important line of research that should be pursued.

Lastly, low- and upper-level circulation fields show that the large-amplitude upper-level trough in mid-latitudes, which extends into the tropics, is a significant feature of cold events. The waves embedded in westerly flow exemplify wintertime tropical-extratropical interactions, leading

to cooling in southeastern South America, as detected by observations in central South America.

The year 2021 was particularly intense in terms of extreme climatic events in tropical South America. In addition to the cold wave described in this study, an unusually large flood was reported in the northern and central Amazon basin in June 2021. Extreme drought conditions characterized southern Brazil. Both hydroclimatic events are related to an intensified continental Hadley Cell (Espinoza et al. 2022; Rao et al. 2022).

Supplementary Information The online version contains supplementary material available at https://doi.org/10.1007/s00382-023-06701-1.

Acknowledgements This work was supported by the National Institute of Science and Technology for Climate Change Phase 2 under CNPq Grant 465501/2014-1; FAPESP Grants 2014/50848-9, and the National Coordination for Higher Education and Training (CAPES) Grant 88887.136402-00INCT. JCE and JPS have been supported by the French AMANECER-MOPGA project funded by ANR and IRD (ANR-18-MPGA-0008).

Author contributions JM: conceptualization; funding acquisition; investigation; methodology; supervision; writing—original draft; writing—review and editing. JCE and MLB: conceptualization; formal analysis; investigation; methodology; visualization; writing—original draft; writing—review and editing. APC: conceptualization; formal analysis; investigation; methodology; software; visualization. AMR: data curation; formal analysis; methodology; software; validation; visualization. MS: data curation; formal analysis; methodology; software; validation; visualization. JMC, JPS, and KC: data curation; formal analysis; methodology; validation; visualization. RS: data curation; synoptic analysis; methodology; software; validation; visualization.

Funding This study was funded by Conselho Nacional de Desenvolvimento Científico e Tecnológico (Grant no. Grant 465501/2014-1) and Fundação de Amparo à Pesquisa do Estado de São Paulo (Grant no. 2014/50848-9).

Data availability Climatic data is freely available from the national meteorological services of the participant countries.

Declarations

Conflict of interest The authors declare having no competing interests.

Ethics approval and consent to participate The study included human or animal subjects and all authors approved the study and manifested their consent in participating in the elaboration and production of this article.

Consent for publication All authors manifested their consent for publication.

References

Alexander LV, Zhang X, Peterson TC, Caesar J, Gleason B, Klein Tank AMG, Haylock M, Collins D, Trewin B, Rahimzadeh F, Tagipour A, Rupa Kumar K, Revadekar J, Griffiths G, Vincent L, Stephenson DB, Burn J, Aguilar E, Brunet M, Taylor M, New M, Zhai P, Rusticucci M, Vazquez-Aguirre JL (2006) Global observed changes in daily climate extremes of temperature and precipitation. J Geophys Res 111:D05109. https://doi.org/10.1029/2005JD006290

Alvarez MS, Vera CS, Kiladis GN, Liebmann B (2016) Influence of the Madden–Julian oscillation on precipitation and surface air temperature in South America. Clim Dyn 46:245–262

Ambrizzi T, Hoskins BJ (1997) Stationary Rossby-wave propagation in a baroclinic atmosphere. Q J R Meteorol Soc 123(540):919–928

Balmaceda-Huarte R, Olmo M, Bettolli ML, Poggi MM (2021) Evaluation of multiple reanalyses in reproducing the spatio-temporal variability of temperature and precipitation indices over southern South America. Int J Climatol. https://doi.org/10.1002/joc.7142

Bazo J, de Perez C, Jacome G, Mantilla K, Destrooper M, Van Aalst M (2021) Anticipation mechanism for cold wave: forecast based financing a case study in the Peruvian Andes. Front Clim 3:747906. https://doi.org/10.3389/fclim.2021.747906

Berntell E, Zhang Q, Chafik L, Körnich H (2018) Representation of multidecadal Sahel rainfall variability in 20th-Century reanalyses. Sci Rep 8(1):6–13. https://doi.org/10.1038/s41598-018-29217-9

Brinkmann WLF, Ribeiro MNG (1972) Air temperatures in Central Amazonia. III.—vertical temperature distribution on a clearcut area and in a secondary forest near Manaus (Cold Front Conditions July 10th. 1969). Acta Amaz 2(3):25–29. https://doi.org/10.1590/1809-43921972023025

Camarinha-Neto GF, Cohen JCP, Dias-Júnior CQ, Sörgel M, Cattanio JH, Araújo A, Wolff S, Kuhn PAF, Souza RAF, Rizzo LV, Artaxo P (2021) The friagem event in the central Amazon and its influence on micrometeorological variables and atmospheric chemistry. Atmos Chem Phys 21:339–356. https://doi.org/10.5194/acp-21-339-2021

Carvalho LMV, Jones C, Ambrizzi T (2005) Opposite phases of the antarctic oscillation and relationships with intraseasonal to interannual activity in the tropics during the Austral summer. J Clim 18:702–718

Ceccherini G, Russo S, Ameztoy Aramendi I, Romero Hernández C, Carmona Moreno C (2016) Magnitude and frequency of Heat and Cold Waves in recent decades: the case of South America. Nat Hazards Earth Syst Sci 16(3):821–831 (**JRC9915**)

Dereczynski C, Chan Chou S, Lyra A, Sondermann M, Regoto P, Tavares P, Chagas D, Gomes JL, Rodrigues DC (2020) Downscaling of climate extremes over South America—Part I: Model evaluation in the reference climate. Weather Clim Extrem 26(29):100273. https://doi.org/10.1016/j.wace.2020.100273

Donat MG, Alexander LV, Yang H, Durre I, Vose R, Dunn RJH, Willett KM, Aguilar E, Brunet M, Caesar J, Hewitson B, Jackl C, Klein Tank AMG, Kruger lAC, Marengo J, Peterson TC, Renom M, Oria Rojas C, Rusticucci M, Salinger J, Elrayah AS, Sekele SS, Srivastava AK, Trewin B, Villarroel C, Vincent LA, Zhai P, Zhang X, Kitching S (2013) Updated analyses of temperature and precipitation extreme indices since the beginning of the Twentieth Century: the HadEX2 dataset. J Geophys Res Atmos. https://doi.org/10.1002/jgrd.50150

Dunn RJH, Alexander LV, Donat MG, Zhang X, Bador M, Herold N, Lippmann T, Allan R, Aguilar E, Aziz Barry A, Brunet M, Caesar J, Chagnaud G, Cheng V, Cinco T, Durre I, de Guzman S, Htay TM, Maisarah V, Ibadullah W, Izzat Bin Ibrahim MK, Khoshkam M, Kruger A, Kubota H, Leng TW, Lim G, Li-Sha L, Mareng J, Mbatha S, McGree S, Menne L, Skansi MM, Ngwenya S, Nkrumah F, Oonariya C, Pabon-Caicedo JD, Panthou G, Pham C, Rahimzadeh F, Ramos AM, Salgado E, Salinger J, Sané Y, Sopaheluwakan A, Srivastava A, Sun Y, Timbal B, Trachow N, Trewin B, van der Schrier G, Vazquez-Aguirre J, Vasquez R, Villarroel C, Vincent L, Vischel T, Vose R, Bin Hj Yussof NAB (2020) Development of an updated global land in situ-based data set of temperature and precipitation extremes: HadEX3. J

Geophys Res Atmos 125:e2019JD032263. https://doi.org/10.1029/2019JD032263
Escobar GH, Mancini Vaz JC, Reboita MS (2019) Circulação Atmosférica em Superfície Associada às Friagens no Centro-Oeste do Brasil Surface Atmospheric Circulation Associated With "Friagens" in Central-West Brazil. Anuário do Instituto de Geociências UFRJ 42(1): 241–254
Espinoza JC, Ronchail J, Lengaigne M, Quispe N, Silva Y, Bettolli ML, Avalos G, Llacza A (2013) Revisiting wintertime cold air intrusions at the east of the Andes: propagating features from subtropical Argentina to Peruvian Amazon and relationship with large-scale circulation patterns. Clim Dyn 41(7–8):1983–2002. https://doi.org/10.1007/s00382-012-1639-y
Espinoza JC, Marengo JA, Schongart J, Jimenez JC (2022) The new historical flood of 2021 in the Amazon River compared to major floods of the 21st century: atmospheric features in the context of the intensification of floods. Weather Clim Extremes. https://doi.org/10.1016/j.wace.2021.100406
Fortune M, Kousky VE (1983) Two severe freezes in Brazil: precursors and synoptic evolution. Mon Weather Rev 111:181–196
Garreaud R (1999) Cold air incursions over subtropical and tropical South America: a numerical case study. Mon Weather Rev 127:2823–2853
Garreaud R (2000) Cold air incursions over Subtropical South America: mean structure and dynamics. Mon Weather Rev 128:2544–2559
Garreaud R, Wallace JM (1998) Summertime incursions of midlatitude air into tropical and subtropical South America. Mon Weather Rev 126:2713–2733
Hamilton M, Tarifa J (1978) Synoptic aspects of a polar outbreak leading to frost in tropical Brazil, July 1972. Mon Weather Rev 106:1545–1556
Hersbach H, Bell B, Berrisford P et al (2020) The ERA5 global reanalysis. Q J R Meteorol Soc 146:1999–2049. https://doi.org/10.1002/qj.3803
Kanno Y et al (2015) Charge and discharge of polar cold air mass in northern hemispheric winter. Geophys Res Lett 42(17):7187–7193
Kiladis GN, Weickmann KM (1992) Circulation anomalies associated with tropical convection during northern winter. Mon Weather Rev 120:1900–1923
Krishnamurti T, Tewari M, Chakraborty D, Marengo J, Silva Dias P, Satyamurty P (1999) Downstream amplification: a possible precursor to major freeze events over southeastern Brazil. Weather Forecast 14:242–270. https://doi.org/10.1175/1520-0434(1999)014,0242:DAAPPT.2.0.CO;2
Lanfredi IS, Camargo R (2018) Classification of extreme cold incursions over South America. Weather Forecast. https://doi.org/10.1175/WAF-D-17-0159.1
Lavaysse C, Cammalleri C, Dosio A, van der Schrier G, Toreti A, Vogt J (2018) Towards a monitoring system of temperature extremes in Europe. Nat Hazard 18:91–104. https://doi.org/10.5194/nhess-18-91-2018
Lindemann DS, Pereira de Freitas RA, Rodrigues JM, Machado DPP, dos Santos EA (2021) Relationship between air masses formed in the Antarctic Region and extreme minimum temperature events in Southern Brazil. Conjecturas 21(5):211–238
Lupo A, Nocera J, Bosart L, Hoffman E, Knight D (2001) South American cold surges: types, composites, and case studies. Mon Weather Rev 129:1021–1041. https://doi.org/10.1175/1520-0493(2001)129,1021:SACSTC.2.0.CO;2
Marengo J (1984) Estudio Sinóptico-Climatico de los Friajes (Friagems) em la Amazon ia Peruana. Revista Forestal Del Peru 12(1–2):1–26
Marengo J, Cornejo A, Satyamurty P, Nobre CA, Sea W (1997a) Cold waves in the South American continent: the strong event of June 1994. Mon Weather Rev 125:2759–2786
Marengo J, Nobre C, Culf A (1997b) Climatic impacts of Friagens in forested and deforested areas of the Amazon Basin. J Appl Met 36:1553–1566
Marengo JA, Ambrizzi T, Kiladis G, Liebmann B (2002) Upper-air wave trains over the Pacific Ocean and wintertime cold surges in tropical-subtropical South America leading to Freezes in Southern and Southeastern Brazil. Theor Appl Climatol 73(3):223–242
Mayta VC, Ambrizzi T, Espinoza JC, Silva Dias PL (2018) The role of the Madden–Julian oscillation on the Amazon Basin intraseasonal rainfall variability. Int J Clim. https://doi.org/10.1002/joc.5810
Mendonça M, Romero H (2012) Ondas de Frio, Indices de Oscilação e impactos socioambientais das variabilidades climáticas de baixa frequência na América do Sul, ACTA Geográfica, Boa Vista, Ed. Esp. Climatol Geogr 185–203
Metz ND, Archambault HM, Srock AF, Galarneau TJ, Bosart LF (2013) A comparison of South American and African preferential pathways for extreme cold events. Mon Weather Rev 141:2066–2086. https://doi.org/10.1175/MWR-D-12-00202.1
Morize H (1922) Contribuição ao Estudo do Clima do Brasil (in Portuguese). Ministério da Agricultura, Industria e Commercio, Observatório Nacional de Rio de Janeiro, 79 pp. [Available from Instituto Nacional de Pesquisas Espaciais, São Jose dos Campos, Caixa Postal 515, São Paulo, Brazil]
Müller GV, Berri GJ (2007) Atmospheric circulation associated with persistent generalized frosts in Central-Southern South America. Mon Weather Rev 135(1268–1289):2007
Müller GV, Ambrizzi T, Nuñez MN (2005) Mean atmospheric circulation leading to generalized frosts in central southern South America. Theor Appl Climatol 82:95–112
Müller GV, Gan MA, Piva ED, Silveira VS (2015) Energetics of wave propagation leading to cold event in tropical latitudes of South America. Clim Dyn 45:1–20. https://doi.org/10.1007/s00382-015-2532-2
Myers V (1964) A cold front invasion in southern Venezuela. Mon Weather Rev 192:513–521
Naumann G, Podesta G, Marengo J, Luterbacher J, Bavera D, Arias Muñoz C, Barbosa P, Cammalleri C, Chamorro L, Cuartas A, de Jager A, Escobar C, Hidalgo C, Leal de Moraes O, McCormick N, Maetens W, Magni D, Masante D, Mazzeschi M, Seluchi M, Skansi MM, Spinoni J, Toreti A (2021) The 2019–2021 extreme drought episode in La Plata Basin, EUR 30833 EN, Publications Office of the European Union, Luxembourg, 2021, ISBN 978-92-76-41898-6 (online). JRC126508. https://doi.org/10.2760/773.
Parmenter F (1976) A Southern Hemisphere cold front passage at the equator. Bull Am Meteorol Soc 57:1435–1440. https://doi.org/10.1175/1520-0477(1976)057%3C1435:ASHCFP%3E2.0.CO;2
Perfect Daily Grind (2021) perfectdailygrind.com/2021/07/why-is-frost-in-brazil-causing-global-coffee-prices-to-increase/. Accessed 16 Mar 2022
Peterson TC, Hoerling MP, Stott PA, Herring S (eds) (2013) Explaining extreme events of 2012 from a climate perspective. Bull Am Meteorol Soc 94(9):S1–S74
Pezza AB, Ambrizzi T (2005) Cold waves in South America and freezing temperatures in São Paulo: historical background (1888–2003) and case studies of cyclones and anticyclones tracks. Rev Bras Meteorol 20:141–158
Prince K, Evans C (2018) A Climatology of extreme South American Andean Cold Surges. J Appl Met Clim 57:2297–2315
Radinović D, Ćurić M (2014) Measuring scales for daily temperature extremes, precipitation and wind velocity. Met Apps 21:461–465. https://doi.org/10.1002/met.1356
Rao VB, Franchito SH, Rosa MB et al (2022) In a changing climate Hadley cell induces a record flood in amazon and another recorded drought across South Brazil in 2021. Nat Hazards 114:1549–1561. https://doi.org/10.1007/s11069-022-05437-1

Reboita MS, Ambrizzi T, da Rocha RP (2009) Relationship between the Southern Annular Mode and Southern Hemisphere atmospheric systems. Revista Brasileira De Meteorologia 24(1):48–55

Reuters (2021) https://www.reuters.com/world/americas/coffee-prices-surge-unusual-cold-threatens-brazilian-production-2021-07-26/#:~:text=Preliminary%20estimates%20from%20the%20Brazilian,country's%20total%20arabica%20crop%20area. Accessed 1 Mar 2022

Ricarte RMD, Herdies DL, Barbosa TF (2015) Review: patterns of atmospheric circulation associated with cold outbreaks in southern Amazonia. Meteorol Appl 22:129–140

Roberts J, Roberts TD (1978) Use of the Butterworth low-pass filter for oceanographic data. J Geophys Res 83(C11):5510–5514. https://doi.org/10.1029/jc083ic11p05510

Segura H, Espinoza JC, Junquas C, Lebel T, Vuille M, Garreaud R (2020) Recent changes in the precipitation-driving processes over the southern tropical Andes/western Amazon. Clim Dyn 54(5):2613–2631

Segura H, Espinoza JC, Junquas C, Lebel T, Vuille M, Condom T (2022) Extreme austral winter precipitation events over the South-American Altiplano: regional atmospheric features. Clim Dyn. https://doi.org/10.1007/s00382-022-06240-1

Seneviratne SI, Zhang X, Adnan M, Badi W, Dereczynski C, Di Luca A, Ghosh S, Iskandar I, Kossin J, Lewis S, Otto F, Pinto I, Satoh M, Vicente-Serrano SM, Wehner M, Zhou B (2021) Weather and Climate Extreme Events in a Changing Climate. In: Masson-Delmotte V, Zhai P, Pirani A, Connors SL, Péan C, Berger S, Caud N, Chen Y, Goldfarb L, Gomis MI, Huang M, Leitzell K, Lonnoy E, Matthews JBR, Maycock TK, Waterfield T, Yelekçi O, Yu R, Zhou B (eds) Climate Change 2021: the physical science basis. Contribution of working group I to the sixth assessment report of the intergovernmental panel on climate change. Cambridge University Press (**in press**)

Serra A, Ratisbona L (1942) As massas de ar da America do Sul (in Portuguese). Ministerio da Agricultura, Servico de Meteorologia, Rio de Janiero. [Available from Instituto Nacional de Pesquisas Espaciais, São Jose dos Campos, Caixa Postal, São Paulo, Brazil]

Sicart JE, Espinoza JC, Queno L, Medina M (2015) Radiative properties of clouds over a tropical Bolivian glacier: seasonal variations and relationship with regional atmospheric circulation. Int J Climatol. https://doi.org/10.1002/joc.4540

Skansi M, Brunet M, Sigró J, Aguilar E, Arevalo Groening JA, Bentancur OJ, Castellón Geier YR, Correa Amaya RL, Jácome H, Malheiros Ramos A, Oria Rojas C, Pasten AM, Sallons Mitro S, Villaroel Jiménez C, Martínez R, Alexander LV, Jones PD (2013) Warming and wetting signals emerging from analysis of changes in climate extreme indices over South America. Glob Planet Change 100:295–307. https://doi.org/10.1016/j.gloplacha.2012.11.004

Sulca J, Vuille M, Roundy OP, Takahashi K, Espinoza JC, Silva Y, Trasmonte G, Zubieta R (2018) Climatology of extreme cold events in the central Peruvian Andes during austral summer: origin, types and teleconnections. Q J R Meteorol Soc 2018:1–22

Swiss Info (2021) https://www.swissinfo.ch/spa/bolivia-inviernobolivia-registra-las-temperaturas-m%C3%A1s-bajas-en-lo-que-va-de-este-invierno/46749846. Accessed 7 Mar 2022

Vera C, Vigliarolo P (2000) Diagnostic study of cold-air outbreaks over South America. Mon Weather Rev 128:3–24

Willis EO (1976) Effects of a cold wave on an Amazonian avifauna in the upper Paraguay drainage, Western Mato Grosso, and suggestions on Oscine-Suboscine relationships. Acta Amaz 6(3):379–394

WMO (2015) Guidelines on the Definition and Monitoring of Extreme Weather and Climate Events; TT-DEWCE. 4/14/2016 Technical Report; World Meteorological Organization, Geneva

WMO (2022) State of Climate in Latin America and the Caribbean 2021. World Meteorological Organization: Geneva, Switzerland. WMO-No. 1295

Yu Y et al (2015) Relationship between warm airmass transport into the upper polar atmosphere and cold air outbreaks in winter. J Atmos Sci 72(1):349

Zeng N, Yoon JH, Marengo JA, Subramaniam A, Nobre CA, Mariotti A, Neelin JD (2008) Causes and impacts of the 2005 Amazon drought. Environ Res Lett 3(1):014002. https://doi.org/10.1088/1748-9326/3/1/014002